The phosphorylation of RPS6 S235/236 in JHH-2, SNU-423, and SNU-387 cells was insensitive to sorafenib (Fig. 3*C*). However, the active MAPK pathway in these cell lines seems to lie downstream of RAF kinases. An MEK inhibitor, CI-1040 (Fig. 3*B*), enhanced the attenuation of p-RPS6 S235/236 by everolimus in JHH-2 and SNU-423 cells (Fig. 4*B*), and an RSK inhibitor, SL0101, enhanced the attenuation of p-RPS6 S235/236 by everolimus in JHH-2 and SNU-387 cells (Fig. 4*B*).

Marked inhibition of p-RPS6 S235/236 by combined blockade of the MAPK pathway downstream of RAF and the mTOR pathway prompted us to examine the effect of this drug combination on HCC cell growth. CI-1040 had no inhibitory effect on the growth of SNU-423 cells at a concentration of 0.1 μM (Fig. 4*C*), but it was able to enhance the growth-inhibitory effect of AZD8055 (Fig. 4*D*). Synergy between AZD8055 and CI-1040 was confirmed via Chou–Talalay median dose effect analysis (17) (supplemental Table S8). The combination index values at 50%, 75%, and 90% growth inhibition were 0.783, 0.804, and 0.827, respectively (values of <1 are defined as representative of synergistic effects). These results suggest that HCC patients refractory to sorafenib with a high level of p-RPS6 S235/236 might be treatable with an mTOR inhibitor in combination with drugs that block the MAPK signaling pathway.

To further provide a rational basis for synergistic targeting of the mTOR and MAPK pathways in HCC, we performed unsupervised hierarchical cluster analysis of 23 HCC cell lines based on their phosphorylation status of signaling components in the mTOR and MAPK pathways listed in supplemental Table S9. Clustering analysis stratified the cell lines into two major groups, A and B (supplemental Fig. S1). In comparison with group A, group B showed higher levels of phosphorylated MAPK signaling components including p-PDGF receptor-β(Thr751), p-Raf-A(Ser299), and phosphorylated signaling modules of the JNK and p38 MAPK pathways (supplemental Fig. S1, C1). Among them, the levels of p-p53 at Ser392, Ser37, and Ser6 differed substantially between groups A (low) and B (high) (supplemental Fig. S1). In addition, cell lines clustered into group A tended to have simultaneous phosphorylation of the mTOR signaling components C2, RPS6(Ser235/236), RPS6(Ser240/244), and eIF4G(Ser1108) (supplemental Fig. S1). With some notable exceptions, sorafenib-insensitive cell lines (high IC_{50} values for sorafenib) and sorafenib-sensitive cell lines (low IC_{50} values for sorafenib) were clustered into group A and group B, respectively. Although sorafenib-insensitive SNU-387, JHH-1, and KIM-1 cells were classified into the sorafenib-sensitive group B, their phosphorylation levels of mTOR signaling components C2 were higher than those in the other cell lines in group B, suggesting that activation of mTOR signaling might be responsible for the resistance to sorafenib in these cell lines. Some of the sorafenib-insensitive cell lines (*e.g.* Alexander, JHH-2, and SNU-475 cells) partitioned into subtype Ab (supplemental Fig. S1) were characterized by prominent activation of mTOR signaling components C2 and MAPK signaling components C1. Together, these findings imply that there is a certain population of HCC cells showing up-regulation of both mTOR and MAPK signaling. Such an HCC subtype might respond better to combination treatment with mTOR and MAPK inhibitors. When we compared the phosphorylation status of the mTOR and MAPK signaling nodes in 95 cell lines by means of unsupervised hierarchical clustering, HCC cell lines were significantly clustered together ($p = 0.011$ by Fisher's exact test) in group A (supplemental Fig. S2), characterized by high levels of phosphorylation of the signaling components C1 and C2, in comparison to cell lines derived from seven other cancer types (supplemental Table S10). The signaling components C1 included previously reported targets of sorafenib such as b-RAF and PDGF receptor-β, as well as the upstream modules of the mTOR pathway (*e.g.* Akt and PDK). The components C2 comprised RPS6(Ser235/236), RPS6(Ser240/244), eIF4G(Ser1108), and the signaling modules of the JNK and p38 MAPK pathways. These observations may reflect the fact that the activation of MAPK signaling by itself, or in combination with mTOR signaling, is a unique feature of HCC.

It is noteworthy that some sorafenib-sensitive and -insensitive cell lines were clustered together into subgroup Aa (supplemental Fig. S1). Although this subgroup was characterized by relatively low levels of both mTOR and MAPK signaling activation, the most sorafenib-sensitive cell line, SNU-449, was classified into this subgroup. It is therefore plausible that some other signaling pathway, in addition to the mTOR and MAPK pathways, may be involved in defining the marked sensitivity of SNU-449 cells to sorafenib.

DISCUSSION

Derangements in the phosphorylation of signaling molecules are hallmarks of cancers, and are often considered as targets of molecular therapies. By profiling the phosphorylation status of multiple signaling components, it is possible to derive important clues for understanding the pathogenesis and classification of cancers. In this study, a high level of p-RPS6 S235/236 was detected in sorafenib-resistant HCC cells. Consistent with this *in vitro* observation, such high expression of p-RPS6 S235/236 was detected in pretreatment biopsy specimens from HCC patients who had shown early radiographically evident disease progression after starting sorafenib therapy. The number of patient samples analyzed in this study was small and insufficient for providing conclusive evidence, but the present findings warrant future clinical studies to evaluate the significance of p-RPS6 S235/236 as a predictor of response to sorafenib. In order to ensure accurate validation of the utility of p-RPS6 S235/236 as a predictor in future studies, standardized guidelines of immunohistochemistry for detecting p-RPS6 (Ser235/236) need to be developed, including tissue preparation, fixation, staining methods, scoring system, and the definition of a "positive" result.

p-RPS6 has been used as a molecular surrogate for mTOR activation. Villanueva *et al.* (22) assessed 314 surgical specimens of HCC immunohistochemically using an anti-p-RPS6 S240/244 antibody. They detected p-RPS6 S240/244 in half of the cases examined, and positive staining was correlated with HCC recurrence (22). Although antibodies against p-RPS6 S235/236 and p-RPS6 S240/244 have been used equivalently in many studies to evaluate mTOR activation (22, 23), the phosphorylation of these serine residues was found to be differentially regulated (Fig. 2*A*). An earlier study demonstrated persistent phosphorylation of RPS6 S235/236 in cells derived from S6K1$^{-/-}$/S6K2$^{-/-}$ double-knockout mice, and it was concluded that this paradoxical phosphorylation was caused by MAPK signaling. A later study revealed that RSK (MAPK pathway) predominantly phosphorylated the serine 235 and 236 residues of RPS6, whereas S6K (mTOR pathway) broadly phosphorylated the serine 235, 236, 240, 244, and 247 residues. Therefore, use of an antibody against p-RPS6 S240/244 would seem more appropriate for specific detection of the mTOR pathway activation status (20). In the present study, however, we found that phosphorylation of the serine 235 and 236 residues of RPS6 reflected cross-talk between the mTOR and MAPK pathways (Fig. 3*C*) and served as a predictive biomarker of sorafenib sensitivity. Although RAF kinases (MAPK pathway) are one of the main molecular types targeted by sorafenib, intervention of active mTOR signaling in the MAPK pathway seems to be one of the molecular mechanisms responsible for the resistance of HCC to sorafenib.

It is therefore conceivable that HCC patients with tumors having high levels of p-RPS6 S235/236 could benefit from inhibition of mTOR signaling. We found that mTOR inhibitors showed greater antitumor activity against sorafenib-resisntant HCC cells (Fig. 3*E*). A recent phase I/II study of everolimus given daily as a single agent in patients with advanced HCC showed that the drug was well tolerated and exerted preliminary antitumor activity in some patients (24). A phase III EVOLVE-1 randomized trial is now ongoing to evaluate the efficacy of everolimus in HCC patients whose disease progressed during or after sorafenib treatment or who were intolerant to sorafenib (25). This clinical trial is designed to reveal the efficacy of mTOR pathway inhibition for control of sorafenib-resistant HCC and is expected to clarify the significance of our present findings.

Clustering analysis of RPPA data revealed that 6 out of 23 HCC cell lines (Alexander, JHH-2, SNU-475, Huh-7, KIM-1, and JHH-1) had prominent activation of both the MAPK and mTOR pathways, indicating a possible subset of HCC patients who might benefit from a combination of MAPK and mTOR inhibitors (supplemental Fig. S1). We also found synergy between MAPK and mTOR pathway inhibitors in sorafenib-resistant cell lines (Fig. 4). However, there is a need for caution before this can be applied clinically. Activation of MAPK signaling occurred at various levels of RAF/MEK/ERK/RSK in sorafenib-resistant cells (Fig. 3*C*). In addition, clustering analysis showed activation of two other major MAPK pathways, the Jun N-terminal kinase (JNK) and p38 MAPK pathways, in more than half the HCC cell lines (supplemental Fig. S1). Cross-talk among three major MAPK pathways (RAF/MEK/ERK, JNK, and p38MAPK) has been reported previously (26). Together, these findings suggest that careful assessment is vital when selecting an appropriate MAPK inhibitor for each individual HCC patient. Despite extensive sequencing of kinase genes, we were unable to identify any alterations in the pathway that might be responsible, indicating the need to expedite pharmacoproteomics for therapy personalization.

The present study highlighted the potential power of the RPPA platform for pathway profiling. We have provided proof-of-principle support for the utility of the highly sensitive, high-throughput RPPA platform by identifying a practical biomarker with potential clinical applicability. In this study, we used only well-characterized antibodies with high specificity. The Human Antibody Initiative is an ongoing project to raise at least one monospecific antibody against all >20,000 proteins encoded by the human genome (27). It is anticipated that the completion of this project will greatly accelerate the capability of RPPA. The majority of current molecular targeting drugs are designed to target a particular signaling pathway (28). Precise determination of signaling pathways that are activated in individual patients seems to be essential for obtaining maximum benefit from any given treatment. RPPA requires only a minuscule specimen quantity (*e.g.* less than 1 ng of protein per array) and is applicable even to small biopsy samples. The potential clinical utility of RPPA for decision-making and monitoring of cancer therapeutics is thus enormous.

* This work was supported by the National Cancer Center Research and Development Fund (23-A-38 and 23-A-11), the Program for Promotion of Fundamental Studies in Health Sciences conducted by the National Institute of Biomedical Innovation of Japan (10-07, 10-44, and 10-45), and the Research on Biological Markers for New Drug Development conducted by the Ministry of Health, Labor and Welfare of Japan.

[S] This article contains supplemental material.

§ To whom correspondence should be addressed: Mari Masuda, Ph.D., Division of Chemotherapy and Clinical Research, National Cancer Center Research Institute, Tokyo 104-0045, Japan, Tel.: 81-3-3542-2511 (ext. 4251), Fax: 81-3-3547-6045, E-mail: mamasuda@ncc.go.jp.

REFERENCES

1. Ferlay, J., Shin, H. R., Bray, F., Forman, D., Mathers, C., and Parkin, D. M. (2010) Estimates of worldwide burden of cancer in 2008: GLOBOCAN 2008. *Int. J. Cancer* **127,** 2893–2917
2. Llovet, J. M., Ricci, S., Mazzaferro, V., Hilgard, P., Gane, E., Blanc, J. F., de Oliveira, A. C., Santoro, A., Raoul, J. L., Forner, A., Schwartz, M., Porta, C., Zeuzem, S., Bolondi, L., Greten, T. F., Galle, P. R., Seitz, J. F., Borbath, I., Haussinger, D., Giannaris, T., Shan, M., Moscovici, M., Voliotis, D., and Bruix, J. (2008) Sorafenib in advanced hepatocellular carcinoma. *N. Engl. J. Med.* **359,** 378–390
3. Arao, T., Ueshima, K., Matsumoto, K., Nagai, T., Kimura, H., Hagiwara, S., Sakurai, T., Haji, S., Kanazawa, A., Hidaka, H., Iso, Y., Kubota, K.,

Shimada, M., Utsunomiya, T., Hirooka, M., Hiasa, Y., Toyoki, Y., Hakamada, K., Yasui, K., Kumada, T., Toyoda, H., Sato, S., Hisai, H., Kuzuya, T., Tsuchiya, K., Izumi, N., Arii, S., Nishio, K., and Kudo, M. (2013) FGF3/FGF4 amplification and multiple lung metastases in responders to sorafenib in hepatocellular carcinoma. *Hepatology* **57,** 1407–1415

4. Cheng, A. L., Kang, Y. K., Chen, Z., Tsao, C. J., Qin, S., Kim, J. S., Luo, R., Feng, J., Ye, S., Yang, T. S., Xu, J., Sun, Y., Liang, H., Liu, J., Wang, J., Tak, W. Y., Pan, H., Burock, K., Zou, J., Voliotis, D., and Guan, Z. (2009) Efficacy and safety of sorafenib in patients in the Asia-Pacific region with advanced hepatocellular carcinoma: a phase III randomised, double-blind, placebo-controlled trial. *Lancet Oncol.* **10,** 25–34
5. Wilhelm, S. M., Adnane, L., Newell, P., Villanueva, A., Llovet, J. M., and Lynch, M. (2008) Preclinical overview of sorafenib, a multikinase inhibitor that targets both Raf and VEGF and PDGF receptor tyrosine kinase signaling. *Mol. Cancer Ther.* **7,** 3129–3140
6. Abou-Alfa, G. K., Schwartz, L., Ricci, S., Amadori, D., Santoro, A., Figer, A., De Greve, J., Douillard, J. Y., Lathia, C., Schwartz, B., Taylor, I., Moscovici, M., and Saltz, L. B. (2006) Phase II study of sorafenib in patients with advanced hepatocellular carcinoma. *J. Clin. Oncol.* **24,** 4293–4300
7. Ueshima, K., Kudo, M., Takita, M., Nagai, T., Tatsumi, C., Ueda, T., Kitai, S., Ishikawa, E., Yada, N., Inoue, T., Hagiwara, S., Minami, Y., Chung, H., and Sakurai, T. (2011) Des-gamma-carboxyprothrombin may be a promising biomarker to determine the therapeutic efficacy of sorafenib for hepatocellular carcinoma. *Dig. Dis.* **29,** 321–325
8. Hagiwara, S., Kudo, M., Nagai, T., Inoue, T., Ueshima, K., Nishida, N., Watanabe, T., and Sakurai, T. (2012) Activation of JNK and high expression level of CD133 predict a poor response to sorafenib in hepatocellular carcinoma. *Br. J. Cancer* **106,** 1997–2003
9. Nishizuka, S., Charboneau, L., Young, L., Major, S., Reinhold, W. C., Waltham, M., Kouros-Mehr, H., Bussey, K. J., Lee, J. K., Espina, V., Munson, P. J., Petricoin, E., 3rd, Liotta, L. A., and Weinstein, J. N. (2003) Proteomic profiling of the NCI-60 cancer cell lines using new high-density reverse-phase lysate microarrays. *Proc. Natl. Acad. Sci. U.S.A.* **100,** 14229–14234
10. Byers, L. A., Wang, J., Nilsson, M. B., Fujimoto, J., Saintigny, P., Yordy, J., Giri, U., Peyton, M., Fan, Y. H., Diao, L., Masrorpour, F., Shen, L., Liu, W., Duchemann, B., Tumula, P., Bhardwaj, V., Welsh, J., Weber, S., Glisson, B. S., Kalhor, N., Wistuba, I. I., Girard, L., Lippman, S. M., Mills, G. B., Coombes, K. R., Weinstein, J. N., Minna, J. D., and Heymach, J. V. (2012) Proteomic profiling identifies dysregulated pathways in small cell lung cancer and novel therapeutic targets including PARP1. *Cancer Discov.* **2,** 798–811
11. Spurrier, B., Ramalingam, S., and Nishizuka, S. (2008) Reverse-phase protein lysate microarrays for cell signaling analysis. *Nat. Protoc.* **3,** 1796–1808
12. Bolstad, B. M., Irizarry, R. A., Astrand, M., and Speed, T. P. (2003) A comparison of normalization methods for high density oligonucleotide array data based on variance and bias. *Bioinformatics* **19,** 185–193
13. Masuda, M., Maruyama, T., Ohta, T., Ito, A., Hayashi, T., Tsukasaki, K., Kamihira, S., Yamaoka, S., Hoshino, H., Yoshida, T., Watanabe, T., Stanbridge, E. J., and Murakami, Y. (2010) CADM1 interacts with Tiam1 and promotes invasive phenotype of human T-cell leukemia virus type I-transformed cells and adult T-cell leukemia cells. *J. Biol. Chem.* **285,** 15511–15522
14. Li, H., and Durbin, R. (2009) Fast and accurate short read alignment with Burrows-Wheeler transform. *Bioinformatics* **25,** 1754–1760
15. Li, H., Handsaker, B., Wysoker, A., Fennell, T., Ruan, J., Homer, N., Marth, G., Abecasis, G., Durbin, R., and Genome Project Data Processing, S. (2009) The Sequence Alignment/Map format and SAMtools. *Bioinformatics* **25,** 2078–2079
16. Wang, K., Li, M. Y., and Hakonarson, H. (2010) ANNOVAR: functional annotation of genetic variants from high-throughput sequencing data. *Nucleic Acids Res.* 38(16):e164.
17. Chou, T. C. (2010) Drug combination studies and their synergy quantification using the Chou-Talalay method. *Cancer Res.* **70,** 440–446
18. Anjum, R., and Blenis, J. (2008) The RSK family of kinases: emerging roles in cellular signalling. *Nat. Rev. Mol. Cell Biol.* **9,** 747–758
19. Pende, M., Um, S. H., Mieulet, V., Sticker, M., Goss, V. L., Mestan, J., Mueller, M., Fumagalli, S., Kozma, S. C., and Thomas, G. (2004) S6K1(−/−)/S6K2(−/−) mice exhibit perinatal lethality and rapamycin-sensitive 5′-terminal oligopyrimidine mRNA translation and reveal a mitogen-activated protein kinase-dependent S6 kinase pathway. *Mol. Cell. Biol.* **24,** 3112–3124
20. Roux, P. P., Shahbazian, D., Vu, H., Holz, M. K., Cohen, M. S., Taunton, J., Sonenberg, N., and Blenis, J. (2007) RAS/ERK signaling promotes site-specific ribosomal protein S6 phosphorylation via RSK and stimulates cap-dependent translation. *J. Biol. Chem.* **282,** 14056–14064
21. Ascierto, P. A., Kirkwood, J. M., Grob, J. J., Simeone, E., Grimaldi, A. M., Maio, M., Palmieri, G., Testori, A., Marincola, F. M., and Mozzillo, N. (2012) The role of BRAF V600 mutation in melanoma. *J. Transl. Med.* **10,** 85
22. Villanueva, A., Chiang, D. Y., Newell, P., Peix, J., Thung, S., Alsinet, C., Tovar, V., Roayaie, S., Minguez, B., Sole, M., Battiston, C., Van Laarhoven, S., Fiel, M. I., Di Feo, A., Hoshida, Y., Yea, S., Toffanin, S., Ramos, A., Martignetti, J. A., Mazzaferro, V., Bruix, J., Waxman, S., Schwartz, M., Meyerson, M., Friedman, S. L., and Llovet, J. M. (2008) Pivotal role of mTOR signaling in hepatocellular carcinoma. *Gastroenterology* **135,** 1972–1983
23. Zhou, L., Huang, Y., Li, J., and Wang, Z. (2010) The mTOR pathway is associated with the poor prognosis of human hepatocellular carcinoma. *Med. Oncol.* **27,** 255–261
24. Zhu, A. X., Abrams, T. A., Miksad, R., Blaszkowsky, L. S., Meyerhardt, J. A., Zheng, H., Muzikansky, A., Clark, J. W., Kwak, E. L., Schrag, D., Jors, K. R., Fuchs, C. S., Iafrate, A. J., Borger, D. R., and Ryan, D. P. (2011) Phase 1/2 study of everolimus in advanced hepatocellular carcinoma. *Cancer* **117,** 5094–5102
25. Kudo, M. (2011) Signaling pathway and molecular-targeted therapy for hepatocellular carcinoma. *Dig. Dis.* **29,** 289–302
26. Wagner, E. F., and Nebreda, A. R. (2009) Signal integration by JNK and p38 MAPK pathways in cancer development. *Nat. Rev. Cancer* **9,** 537–549
27. Uhlen, M., and Ponten, F. (2005) Antibody-based proteomics for human tissue profiling. *Mol. Cell. Proteomics* **4,** 384–393
28. Wulfkuhle, J. D., Edmiston, K. H., Liotta, L. A., and Petricoin, E. F., 3rd (2006) Technology insight: pharmacoproteomics for cancer—promises of patient-tailored medicine using protein microarrays. *Nat. Clin. Pract. Oncol.* **3,** 256–268

Citation: Clinical and Translational Gastroenterology (2014) 5, e53; doi:10.1038/ctg.2014.5

www.nature.com/ctg

Association of Pancreatic Fatty Infiltration With Pancreatic Ductal Adenocarcinoma

Mika Hori, PhD[1], Mami Takahashi, PhD[2], Nobuyoshi Hiraoka, MD, PhD[3], Taiki Yamaji, MD, PhD, MPH[4], Michihiro Mutoh, MD, PhD[5], Rikako Ishigamori, PhD[5], Koh Furuta, MD, PhD[6], Takuji Okusaka, MD, PhD[7], Kazuaki Shimada, MD, PhD[8], Tomoo Kosuge, MD, PhD[8], Yae Kanai, MD, PhD[3] and Hitoshi Nakagama, MD, DMSc[1,5]

OBJECTIVES: Fatty infiltration (FI) in the pancreas is positively correlated with high body mass index (BMI) or obesity, and the prevalence of diabetes mellitus (DM), which are well-known risk factors of pancreatic cancer. However, the association of FI in the pancreas with pancreatic cancer is unclear. Recently, we have shown that Syrian golden hamsters feature FI of the pancreas, the severity of which increases along with the progression of carcinogenesis induced by a chemical carcinogen. To translate the results to a clinical setting, we investigated whether FI in the pancreas is associated with pancreatic cancer in a series of patients who had undergone pancreatoduodenectomy.

METHODS: In the series, we identified 102 cases with pancreatic ductal adenocarcinoma (PDAC) and 85 controls with cancers except for PDAC. The degree of FI was evaluated histopathologically from the area occupied by adipocytes in pancreas sections, and was compared between the cases and controls.

RESULTS: The degree of FI in the pancreas was significantly higher in cases than in controls (median 26 vs. 15%, $P<0.001$) and positively associated with PDAC, even after adjustment for BMI, prevalence of DM and other confounding factors (odds ratio (OR), 6.1; $P<0.001$). BMI was identified as the most significantly associated factor with FI in the pancreas.

CONCLUSIONS: There is a positive correlation between FI in the pancreas and pancreatic cancer.

Clinical and Translational Gastroenterology (2014) **5,** e53; doi:10.1038/ctg.2014.5; published online 13 March 2014
Subject Category: Pancreas and Biliary Tract

INTRODUCTION

Pancreatic cancer is one of the most lethal human cancers with a 5-year survival rate of <5% in both Japan and the United States.[1] Thus, the development of useful predictive markers for individuals with a high risk of pancreatic cancer would be of great help in detecting pancreatic cancer at its early stages, and might contribute to a significant reduction of mortality. Epidemiological studies have shown that a family history of pancreatic cancer, cigarette smoking, age, obesity, and diseases such as chronic pancreatitis and diabetes mellitus (DM) increase the risk of pancreatic cancer.[2–4] A few pathologic studies of patients with pancreatic cancer have demonstrated fatty infiltraton (FI) in the pancreas parenchyma.[5,6] FI in the pancreas is positively correlated with age, body mass index (BMI), and a history of DM.[7–9]

Recently, we have shown that in Syrian golden hamsters, which exhibit a substantial age-related increase of hypertriglyceridemia and FI in the pancreas, there is further progression of pancreatic FI and carcinogenesis upon treatment with a carcinogen, *N*-nitrosobis (2-oxopropyl) amine (BOP), while the animals are fed a high-fat diet (HFD).[10] Therefore, we hypothesized that FI in the pancreas accompanied by hypertriglyceridemia might be associated with pancreatic cancer in both humans and experimental animals.

In the present case–control study, we examined whether FI in the pancreas is associated with pancreatic ductal adenocarcinoma (PDAC) in humans, independently of several other suggested risk factors for pancreatic cancer, such as obesity and DM.

METHODS

Patients and samples. Between January 2004 and December 2010, 367 patients underwent pancreatoduodenectomy for PDAC at the National Cancer Center Hospital, Japan. Among them, 102 were considered to be appropriate for the present study on the basis of the criteria detailed later. As controls, we used non-cancerous pancreas tissues from 85 patients who had undergone pancreatoduodenectomy for cancer, except for PDAC; these included 46 patients with distal bile duct cancer, 33 with cancer of the ampulla of Vater, 4 with gallbladder cancer, and 2 with duodenal cancer. DM was clinically diagnosed at the referring hospitals, using criteria of fasting blood glucose level ≥126 mg/dl and HbA1c ≥6.1%, before the patients visited our hospital to resect pancreatic cancer. BMI was calculated when the patients were admitted to our hospital. The use of each individual's material for analysis in the

[1]Division of Cancer Development System, National Cancer Center Research Institute, Tokyo, Japan; [2]Central Animal Division, National Cancer Center Research Institute, Tokyo, Japan; [3]Division of Molecular Pathology, National Cancer Center Research Institute, Tokyo, Japan; [4]Epidemiology and Prevention Division, Research Center for Cancer Prevention and Screening, National Cancer Center, Tokyo, Japan; [5]Division of Cancer Prevention Research, National Cancer Center Research Institute, Tokyo, Japan; [6]Division of Pathology and Clinical Laboratories, National Cancer Center Hospital, Tokyo, Japan; [7]Hepatobiliary and Pancreatic Oncology Division, National Cancer Center Hospital, Tokyo, Japan and [8]Hepatobiliary and Pancreatic Surgery Division, National Cancer Center Hospital, Tokyo, Japan
Correspondence: Hitoshi Nakagama, MD, DMSc, National Cancer Center Research Institute, 5-1-1 Tsukiji, Chuo-ku, Tokyo 104-0045, Japan.
E-mail: hnakagam@ncc.go.jp
Received 1 November 2013; revised 6 January 2014; accepted 15 January 2014

present study was approved by the Ethics Review Committee of the National Cancer Center (2010-088). The materials are from patients who had given general consent for the research use of their leftover samples, and all clinical investigations were conducted in accordance with the principles of the Declaration of Helsinki.

Pathological examination. PDACs were examined pathologically and classified according to the World Health Organization classification and TNM classification.[11,12] Surgically resected specimens were fixed in 10% formalin, and the pancreas heads were cut horizontally into serial slices 5 mm thick. In order to evaluate FI appropriately, we conducted a preliminary study to select a target area of pancreas parenchyma in 16 cases of PDAC. As FI is easily affected by any type of pancreatitis associated with cancer infiltration, including obstructive pancreatitis, we selected the FI area for measurement, avoiding any primary and/or secondary effect caused by cancer infiltration (Supplementary Figure S1 online). Thus, pancreatitis patients were ruled out from the FI evaluation. First, we selected anterior and cranial areas of the pancreas near the duodenum that correspond to the dorsal pancreas during organogenesis. Second, we chose areas of the pancreas near the ampulla of Vater if the former area was affected by cancer infiltration. If both of these areas were affected by cancer infiltration, such cases were excluded from the study. Thus, we selected one section containing non-tumorous pancreatic tissue and confirmed whether it fulfilled the above conditions. Then, FI areas were measured quantitatively as the percentage of area infiltrated by adipocytes relative to the total area on the section was calculated using the WinROOF image analysis software package (Mitani Corp, Tokyo, Japan). The reproducibility of this quantitation method was checked preliminarily by comparing the FI area of one section with another section derived from tissue immediately adjacent to the former. The difference between the two FI area values measured in 16 pairs of sections was 5.6% on average.

Serum sample collection and assays. Peripheral blood was collected from each patient at the time of the hospital visit prior to treatment, and blood sugar, HbA1c, and serum levels of total cholesterol (TC), high-density lipoprotein (HDL), amylase, CEA, and CA19-9 were measured by participants at the National Cancer Center Hospital. For further examination, serum provided by the National Cancer Center Biobank, Japan, was stored at −20°C. Serum adiponectin, leptin and insulin growth factor-I (IGF-I) (R&D Systems, Inc., Minneapolis, MN, USA), apolipoprotein A-II (apoA-II) (Assay pro, St Charles, MO, USA), insulin (Millipore, Billerica, MA, USA), and serum amyloid A (SAA; Invitrogen, Camarillo, CA, USA) were measured using enzyme-linked immunosorbent assay kits in accordance with the manufacturers' instructions. The levels of serum triglycerides (TGs), HDL, and gamma-glutamyltransferase (GGT) were analyzed using the FUJI Dri-Chem system (Fuji Film, Tokyo, Japan).

Statistical analysis. The cases and controls were classified into three subgroups, $<10\%$, 10–20%, and $\geq 20\%$, according to the area of FI. The cutoff points of 10 and 20 were nearly equal to the tertile cutoff points in the controls, namely 9.5 and 20.4. An unconditional logistic regression model was used to estimate odds ratios (ORs) and their 95% confidence intervals (CIs) of PDAC according to the three categories of FI in the pancreas, the lowest value being used as a reference. Two-sided P values <0.05 were considered to indicate statistical significance. All statistical analyses were carried out using the Statistical Analysis System (SAS), version 9.1 software package (SAS Institute, Cary, NC, USA) by a statistician (T.Y.).

RESULTS

Patient characteristics. Among 102 cases, one was classified as stage IB, 27 as stage IIA, 65 as stage IIB, and 9 as stage IV. The characteristics of the case and control patients are summarized in Table 1. Controls were older than cases ($P=0.001$), and there was a male predominance in both groups. The known risk factors for PDAC were compared between cases and controls. The prevalence of DM ($P=0.03$) and family history of pancreatic cancer ($P=0.007$) in cases was higher than in controls. The values of blood sugar ($P=0.002$) and HbA1c ($P<0.001$) in cases were also significantly higher than in the controls. The serum apoA-II level was shown to be lower in cases than in controls ($P=0.02$), as reported previously, in comparison with healthy subjects. CEA ($P=0.04$) and CA19-9 ($P<0.001$), serum tumor markers for PDAC, were also significantly higher in cases than in controls. Meanwhile, serum levels of GGT ($P<0.001$), which are associated with liver and biliary disorders, were higher in controls than in cases.

Association of FI in the pancreas with PDAC. In the human pancreas, adipocytes were observed to accumulate in the area between pancreatic lobules (interlobular fat), especially around great vessels, or to be scattered in the lobules (intralobular fat), as shown in Figure 1. The distribution pattern of FI in some patients was similar to that observed in hamster pancreas.[10] In this study, FI in the pancreas was defined as the sum of the areas showing any types of FI in the pancreas parenchyma. Table 1 shows that the area of FI in the pancreas was significantly greater in cases than in controls (median 26 vs. 15%, $P<0.001$). Types of differentiation and stages of PDACs were not associated with the degree of FI (data not shown).

Table 2 shows the association between the area of FI in the pancreas and PDAC. A significantly higher OR for PDAC was observed according to the area of FI in the pancreas ($P<0.001$). Adjusted for sex, age, BMI, history of DM, and family history of pancreatic cancer, confounding factors for pancreatic cancer, ORs for PDAC showed an increasing trend according to the area of FI ($P<0.001$). Even when patients with a BMI $>25\ kg/m^2$, a history of DM, and a family history of pancreatic cancer were excluded, positive associations between the degree of FI in the pancreas and PDAC were observed ($P<0.001$ overall).

The factors associated with FI. The characteristics of the study participants were examined in relation to the degree of FI of the pancreas in controls and cases and are shown in Supplementary Tables 1 and 2, respectively. BMI and age were positively correlated with the area of FI of the pancreas

Table 1 Selected characteristics of study subjects

Characteristic	Cases ($n=102$)	Controls ($n=85$)	P^a
Categorical variables, n *(%)*			
FI in the pancreas ≥ 20%	64 (62.7)	30 (35.2)	<0.001
Male	60 (58.8)	60 (70.5)	0.12
Ever smoking	53 (51.9)	42 (49.4)	0.77
Frequent drinking (5–7 times/week)	34 (33.3)	31 (36.9)	0.85
DM	30 (29.4)	14 (16.4)	0.03
Hypertension	36 (35.2)	27 (31.7)	0.64
Hyperlipidemia	7 (6.8)	10 (11.7)	0.30
Family history of PC	11 (10.7)	1 (1.1)	0.007
Continuous variables, median (IQR)			
FI in the pancreas, %	25.8 (14.2–40.9)	15.0 (7.7–24.8)	<0.001
Age, years	63.5 (56–69)	68.0 (63–73)	0.001
BMI, kg/m^2	22.4 (20.3–24.3)	22.7 (20.7–24.2)	0.95
Blood sugar, mg/dl	114.0 (100–141)	106.0 (93–119)	0.002
HbA1c, %	5.5 (5.1–6.4)	5.1 (4.7–5.5)	<0.001
TC, mg/dl	189.0 (162–221)	195.0 (169–227)	0.31
HDL, mg/dl	52.0 (43–62)	52.0 (42–67)	0.47
TG, mg/dl	149.0 (109–209)	155.0 (117–210)	0.38
Apo A-II, μg/ml	219.3 (136.7–397.5)	327.3 (174.0–444.4)	0.02
Adiponectin, μg/ml	5.4 (3.0–9.6)	6.3 (3.2–12.3)	0.37
Leptin, ng/ml	3.2 (2.2–4.6)	3.1 (2.4–3.8)	0.57
Insulin, mU/l	3.5 (2.5–5.8)	3.7 (2.8–6.4)	0.41
IGF-I, ng/ml	69.7 (53.2–93.5)	74.1 (54.4–96.4)	0.69
Amylase, IU/l	107.0 (75–182)	105.0 (83–141)	0.55
CEA, ng/ml	2.6 (1.6–4.1)	2.0 (1.3–3.4)	0.04
CA19-9, U/ml	96.0 (46–400)	30.0 (16–121)	<0.001
SAA, μg/ml	22.1 (8.93–54.3)	35.8 (12.7–89.8)	0.06
GGT, ng/ml	105.0 (33–311)	339.0 (101–673)	<0.001

Apo A-II, apolipoprotein A-II; BMI, body mass index; DM, diabetes mellitus; FI, fatty infiltration; GGT, gamma-glutamyltransferase; HDL, high density lipoprotein; IGF-I, insulin growth factor-I; IQR, interquartile range; PC, pancreatic cancer; SAA, serum amyloid A; TC, total cholesterol; TG, triglyceride.
[a]Based on the Fisher's exact test for percentage difference and the Wilcoxon rank-sum test for median difference.

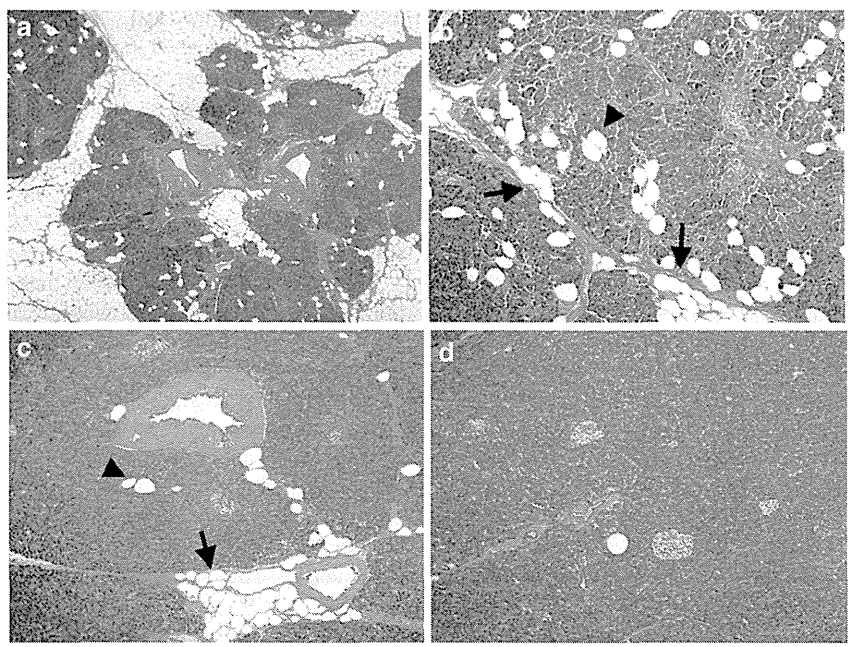

Figure 1 Histology of the human pancreas with fatty infiltration. (**a**, **b**) Pancreas tissue with moderate to severe FI. Most of the pancreas parenchyma has been replaced by adipocytes, and the remaining pancreas lobules resemble islets surrounded by a fatty lake. Most adipocytes have accumulated interlobularly (arrow in **b**), but some are scattered within the lobules (arrowhead in **b**). (**c**) Pancreas tissue with mild FI. Adipocytes have accumulated around arterioles (arrow), and several adipocytes are scattered within the lobules (arrowhead). (**d**) Pancreas tissue with minimal FI. Super-low magnification in **a**, and low magnification in (**b** to **d**).

Table 2 Association of the degree of FI in the pancreas with pancreatic ductal adenocarcinoma

	FI in the pancreas						
	<10%		≥10%, <20%		≥20%		
Population	**OR**	**95% CI**	**OR**	**95% CI**	**OR**	**95% CI**	***P*[a]**
All subjects							
Cases/controls		17/30		21/25		64/30	
Crude estimate	1	Reference	1.4	(0.6–3.4)	3.7	(1.8–7.8)	<0.001
Adjusted estimate[b]	1	Reference	2.3	(0.8–6.2)	6.1	(2.4–15.2)	<0.001
Excluding those with BMI of ≥25 kg/m²							
Cases/controls		17/28		18/22		49/24	
Adjusted estimate[c]	1	Reference	2.1	(0.7–5.9)	6.3	(2.4–16.5)	<0.001
Excluding those with past history of DM							
Cases/controls		14/28		18/21		40/22	
Adjusted estimate[d]	1	Reference	3.1	(1.0–9.3)	7.5	(2.6–21.3)	<0.001
Excluding those with family history of PC							
Cases/controls		15/29		17/25		59/30	
Adjusted estimate[e]	1	Reference	2.0	(0.7–5.5)	5.4	(2.2–13.6)	<0.001

BMI, body mass index; CI, confidence interval; DM, diabetes mellitus; FI, fatty infiltration; OR, odds ratio; PC, pancreatic cancer.
[a]Statistical tests for trend (two-sided) were assessed by assigning ordinal values to the degree of FI in the pancreas.
[b]Adjusted for sex, age (≤60, 61–70 and >70), BMI (<25, ≥25), past history of DM (yes or no) and family history of PC (yes or no).
[c]Adjusted for sex, age (≤60, 61–70 and >70), past history of DM (yes or no), and family history of PC (yes or no).
[d]Adjusted for sex, age (≤60, 61–70 and >70), BMI (<25, ≥25), and family history of PC (yes or no).
[e]Adjusted for sex, age (≤60, 61–70 and >70), BMI (<25, ≥25), and past history of DM (yes or no).

in both cases and controls. In control patients, the serum TG and amylase values were also positively correlated with the area of FI in the pancreas. Meanwhile, the levels of the serum insulin, HbA1c and blood sugar in case patients were positively correlated with the area of FI in the pancreas. To further investigate an association with FI in the pancreas, we conducted a multivariable linear regression analysis in each group, in which the above variables (BMI, serum TG, and amylase for controls; BMI, serum insulin, HbA1c, and blood sugar for cases), as well as age and sex, were included in one model. After mutual adjustment, a statistically significant association was noted only for BMI (controls, $P=0.001$; cases, $P=0.01$).

DISCUSSION

Based on epidemiological observation of human pancreatic cancers, FI in the pancreas was suggested to associate with PDAC, independently of known risk factors such as obesity and DM (Supplementary Figure S2). Although we identified BMI, a measurement of obesity, as the most significantly associated factor among several factors related to FI in the pancreas, FI in the pancreas was likely to increase the risk of pancreatic cancer beyond the effect of obesity alone. Some previous studies have evaluated pancreatic FI in humans using diagnostic modalities such as ultrasound, magnetic resonance imaging, or magnetic resonance spectroscopy.[9,13–16] FI in the pancreas has been suggested to promote dissemination and lethality of PDAC and to increase the risk of postoperative pancreatic fistula.[17,18] Here we demonstrated that the area of FI in histopathological sections of PDAC resected can be used as a quantitative indicator of the degree of FI. This is the first report to indicate an association between the area of FI and the development of PDAC.

Although mechanistic insights into how PDAC could develop from such an adipocyte-rich microenvironment are not clear, recent evidence suggests that ectopic fat accumulation produces certain adipocytokines that induce cell proliferation.[19,20] Serum adipocytokine levels were not clearly correlated with the area of FI in the present study, but the level of leptin expression was high in the pancreas of BOP-treated hamsters fed a HFD.[10] Thus, local release of adipocytokines from adipocytes in an adipocyte-rich microenvironment appeared to be correlated with PDAC development.

In the present study, serum insulin levels in cases were positively correlated with FI in the pancreas. It has also been reported that HOMA-IR is strongly correlated with FI of the pancreas except in subjects with a history of DM, pancreatic diseases and liver diseases.[9] In an *in vitro* setting, it has been shown that glucose-dependent insulinotropic polypeptide activates lipoprotein lipase, leading to TG accumulation in differentiated 3T3-L1 adipocytes in the presence of insulin.[21] Therefore, it is conceivable that induction of high glucose and insulin levels by hyperphagia could be associated with FI through activation of lipoprotein lipase in the pancreas. Conversely, it has also been suggested that increased pancreatic FI is related to β-cell dysfunction in the absence of type 2 DM,[22] and that this can lead to subsequent development of type 2 DM.[23,24] The hyperinsulinemia seen in human obesity, including the early phase of type 2 DM, may be closely related to FI in the pancreas.

Several possible mechanisms underlying the development of FI in the pancreas can be speculated. It has been shown in experimental animal models that FI can be induced in the pancreas by obstruction of the pancreatic duct or vasculature.[25,26] Smits and van Geenen[27] have showed that FI or non-alcoholic fatty pancreas disease represents fat accumulation induced by obesity and metabolic syndrome, while fatty replacement represents replacement of adipocytes induced by

death of acinar cells. We agree with their statements that pancreatic fat accumulation is mainly induced by these two factors. In this study, pancreatic FI in cases represents any type of fat accumulation caused by any type of etiology. It has been reported that lipotoxicity caused by a high TG content induces inflammatory responses and necrosis in pancreatic acinar cells *in vitro*.[28,29] It has also been shown that c-Myc activity is required for growth and maturation of the exocrine pancreas and for the transdifferentiation of acinar cells into adipocytes in mice.[30] Thus, pancreas containing scattered adipocytes might be more sensitive to acinar cell damage due to lipotoxity and other genetic factors, and scattered FI may reflect the acinar cell death or transdifferentiation after the damage.

Some limitations could be pointed out in this study. The major limitation is that it lacked normal healthy controls because pancreatic sections could be obtained only from patients who had undergone pancreatoduodenectomy. A second limitation is that we could not measure FI in more than one pancreatic section, as areas for measuring FI were limited and small because the areas of tumor and secondary inflammation were avoided. Therefore, a future study using a non-invasive method will be required to evaluate FI in a large area/volume of pancreas from healthy and case subjects. Previously, we have reported a case of PDAC that was associated with marked FI in the pancreas, as seen on computed tomography images.[31] Computed tomography imaging of the pancreas would be a useful approach for accurate evaluation and follow-up of pancreatic FI in normal subjects, as well as in cohort studies. The third limitation is that we did not exclude the areas of pancreas with PanINs from the sections for measuring FI because it is known that PanINs are sometimes found in pancreatic tissue of the elderly, and also that a large number of PanINs with various grades are found in the pancreas of the patients with PDAC. Therefore, it is extremely difficult to measure FI in the pancreas tissue without PanINs, especially in the limited area for measuring FI. The fourth limitation is that BMI could be underestimated in the cases, because weight loss is a very common symptom of patients suffering from pancreatic cancer even though most cases were classified as stage IIA or IIB. The fifth limitation is that there is no validation study. To confirm the observation in the present study, the same study should be repeated with the same methods in another center (hospital/institution). The final limitation is that we cannot distinguish whether FI was a risk factor or a consequence of the cancer. The only way to demonstrate that FI is a risk factor for PDAC is to perform a prospective cohort study to observe whether individuals with fatty pancreas could develop PDAC. For this purpose, we are now trying to establish the methods to evaluate FI in a large area/volume of pancreas by non-invasive method, using computed tomography and magnetic resonance imaging. In addition, studies on pancreatic carcinogenesis using animal models of fatty pancreas would be helpful to elucidate underlying mechanisms.

In conclusion, there is a positive correlation between FI in the pancreas and pancreatic cancer. The development of effective detection methods and/or markers of FI, especially "fatty pancreas" with severe FI, is warranted for mass screening of individuals at high risk of pancreatic cancer at health examinations.

CONFLICT OF INTEREST

Guarantor of the article: Hitoshi Nakagama, MD, DMSc.

Specific author contributions: Mika Hori contributed to the design of the study, acquisition, analysis and interpretation of data, writing and drafting of the manuscript; Mami Takahashi contributed to the conception of the study, development of methodology and data analysis and revision of the manuscript; Nobuyoshi Hiraoka contributed to the histopathological analysis and revision of the manuscript; Taiki Yamaji contributed to the statistical analysis and revision of the manuscript; Michihiro Mutoh contributed to data analysis and revision of the manuscript; Rikako Ishigamori contributed to the histopathological analysis; Koh Furuta contributed to material supports in human serum analysis; Takuji Okusaka contributed to the clinical revision of the manuscript; Kazuaki Shimada contributed to the clinical revision of the manuscript; Tomoo Kosuge contributed to the clinical revision of the manuscript; Yae Kanai contributed to the histopathological analysis; Hitoshi Nakagama contributed to study supervision and revision of the manuscript.

Financial support: This work was supported by: Grants-in-Aid for Cancer Research from the Ministry of Health, Labour, and Welfare of Japan and Management Expenses Grants from the Government to the National Cancer Center (21–2–1, 23-A-4); a grant of the Third-Term Comprehensive 10-Year Strategy for Cancer Control from the Ministry of Health, Labor, and Welfare of Japan; a grant of the Research Grant of the Princess Takamatsu Cancer Research Fund; Grants-in-Aid from the Foundation for Promotion of Cancer Research and the Pancreas Research Foundation of Japan. M. Hori was an Awardee of Research Resident Fellowships from the Foundation for Promotion of Cancer Research (Japan) and from the Third-Term Comprehensive 10-Year Strategy for Cancer Control during the course of the present research.

Potential competing interests: None.

Acknowledgments. The National Cancer Center Biobank is supported by the National Cancer Center Research and Development Fund, Japan.

Study Highlights

WHAT IS CURRENT KNOWLEDGE

- Fatty infiltration (FI) in the pancreas is positively correlated with obesity and prevalence of DM.
- The association of FI in the pancreas with pancreatic ductal adenocarcinoma (PDAC) is unclear in humans.

WHAT IS NEW HERE

- FI in the pancreas is associated with PDAC development in humans.
- Body masss index (BMI) was identified as the most significantly associated factor with FI in the pancreas.
- FI in the pancreas may increase the risk of PDAC beyond the effect of obesity alone.

1. Maitra A, Hruban RH. Pancreatic cancer. *Annu Rev Pathol* 2008; **3**: 157–188.
2. Patel AV, Rodriguez C, Bernstein L *et al.* Obesity, recreational physical activity, and risk of pancreatic cancer in a large U.S. Cohort. *Cancer Epidemiol Biomarkers Prev* 2005; **14**: 459–466.

3. Huxley R, Ansary-Moghaddam A, Berrington de González A *et al.* Type-II diabetes and pancreatic cancer: a meta-analysis of 36 studies. *Br J Cancer* 2005; **92**: 2076–2083.
4. Li D, Morris JS, Liu J *et al.* Body mass index and risk, age of onset, and survival in patients with pancreatic cancer. *JAMA* 2009; **301**: 2553–2562.
5. Toyama N, Kamiyama H, Suminaga Y *et al.* Pancreas head carcinoma with total fat replacement of the dorsal exocrine pancreas. *J Gastroenterol* 2004; **39**: 76–80.
6. Makay O, Kazimi M, Aydin U *et al.* Fat replacement of the malignant pancreatic tissue after neoadjuvant therapy. *Int J Clin Oncol* 2010; **15**: 88–92.
7. Walters MN. Adipose atrophy of the exocrine pancreas. *J Pathol Bacteriol* 1966; **92**: 547–557.
8. Rosso E, Casnedi S, Pessaux P *et al.* The role of "fatty pancreas" and of BMI in the occurrence of pancreatic fistula after pancreaticoduodenectomy. *J Gastrointest Surg* 2009; **13**: 1845–1851.
9. Lee JS, Kim SH, Jun DW *et al.* Clinical implications of fatty pancreas: correlations between fatty pancreas and metabolic syndrome. *World J Gastroenterol* 2009; **15**: 1869–1875.
10. Hori M, Kitahashi T, Imai T *et al.* Enhancement of carcinogenesis and fatty infiltration in the pancreas in *N*-nitrosobis(2-oxopropyl) amine-treated hamsters by high fat diet. *Pancreas* 2011; **40**: 1234–1240.
11. Hruban RH, Boffetta P, Hiraoka N *et al.* Ductal adenocarcinoma of the pancreas. In: Bosman FT, Carneiro F, Hruban RH, Theise ND (eds). *WHO Classification of Tumours of the Digestive System*. 4th edn. World Health Organization Classification of Tumours IARC: Lyon, France, 2010, pp. 281–291.
12. Sobin LH, Gospodarowicz MK, Wittekind C. *TNM Classification of Malignant Tumours*. Willey-Blackewell: Oxford, UK, 2009.
13. Kovanlikaya A, Mittelman SD, Ward A *et al.* Obesity and fat quantification in lean tissues using three-point Dixon MR imaging. *Pediatr Radiol* 2005; **35**: 601–607.
14. Schwenzer NF, Machann J, Martirosian P *et al.* Quantification of pancreatic lipomatosis and liver steatosis by MRI: comparison of in/opposed-phase and spectral-spatial excitation techniques. *Invest Radiol* 2008; **43**: 330–337.
15. Lingvay I, Esser V, Legendre JL *et al.* Noninvasive quantification of pancreatic fat in humans. *J Clin Endocrinol Metab* 2009; **94**: 4070–4076.
16. Lee SE, Jang JY, Lim CS *et al.* Measurement of pancreatic fat by magnetic resonance imaging: predicting the occurrence of pancreatic fistula after pancreatoduodenectomy. *Ann Surg* 2010; **251**: 932–936.
17. Mathur A, Zyromski NJ, Pitt HA *et al.* Pancreatic steatosis promotes dissemination and lethality of pancreatic cancer. *J Am Coll Surg* 2009; **208**: 989–994.
18. Mathur A, Pitt HA, Marine M *et al.* Fatty pancreas: a factor in postoperative pancreatic fistula. *Ann Surg* 2007; **246**: 1058–1064.
19. Okuya S, Tanabe K, Tanizawa Y *et al.* Leptin increases the viability of isolated rat pancreatic islets by suppressing apoptosis. *Endocrinology* 2001; **142**: 4827–4830.
20. Hardwick JC, Van Den Brink GR, Offerhaus GJ *et al.* Leptin is a growth factor for colonic epithelial cells. *Gastroenterology* 2001; **121**: 79–90.
21. Kim SJ, Nian C, McIntosh CH. Activation of lipoprotein lipase by glucose-dependent insulinotropic polypeptide in adipocytes. A role for a protein kinase B, LKB1, and AMP-activated protein kinase cascade. *J Biol Chem* 2007; **282**: 8557–8567.
22. Tushuizen ME, Bunck MC, Pouwels PJ *et al.* Pancreatic fat content and beta-cell function in men with and without type 2 diabetes. *Diabetes Care* 2007; **30**: 2916–2921.
23. Van Herpen NA, Schrauwen-Hinderling VB. Lipid accumulation in non-adipose tissue and lipotoxicity. *Physiol Behav* 2008; **94**: 231–241.
24. Kahn SE, Hull RL, Utzschneider KM. Mechanisms linking obesity to insulin resistance and type 2 diabetes. *Nature* 2006; **444**: 840–846.
25. Uchida T, Tsuchiya R, Harada N *et al.* Ischemic changes in the pancreas of Watanabe heritable hyper-lipidemic (WHHL) rabbits. *Int J Pancreatol* 1988; **3**: 261–272.
26. Watanabe S, Abe K, Anbo Y *et al.* Changes in the mouse exocrine pancreas after pancreatic duct ligation: a qualitative and quantitative histological study. *Arch Histol Cytol* 1995; **58**: 365–374.
27. Smits MM, van Geenen EJ. The clinical significance of pancreatic steatosis. *Nat Rev Gastroenterol Hepatol* 2011; **8**: 169–177.
28. Navina S, Acharya C, DeLany JP *et al.* Lipotoxicity causes multisystem organ failure and exacerbates acute pancreatitis in obesity. *Sci Transl Med* 2011; **3**: 107–110.
29. Pinnick KE, Collins SC, Londos C *et al.* Pancreatic ectopic fat is characterized by adipocyte infiltration and altered lipid composition. *Obesity* 2008; **16**: 522–530.
30. Bonal C, Thorel F, Ait-Lounis A *et al.* Pancreatic inactivation of c-Myc decreases acinar mass and transdifferentiates acinar cells into adipocytes in mice. *Gastroenterology* 2009; **136**: 309–319.
31. Hori M, Onaya H, Takahashi M *et al.* Invasive ductal carcinoma developing in pancreas with severe fatty infiltration. *Pancreas* 2012; **41**: 1137–1139.

Supplementary Information accompanies this paper on the Clinical and Translational Gastroenterology website (http://www.nature.com/ctg)

Clinical Translational Research

Oncology

Oncology 2014;86:94–103
DOI: 10.1159/000357408

Received: August 27, 2013
Accepted: November 8, 2013
Published online: January 18, 2014

MicroRNA Expression and Functional Profiles of Osteosarcoma

Eisuke Kobayashi[a, b] Reiko Satow[a] Masaya Ono[a] Mari Masuda[a]
Kazufumi Honda[a] Tomohiro Sakuma[c] Akira Kawai[d] Hideo Morioka[b]
Yoshiaki Toyama[b] Tesshi Yamada[a]

[a]Division of Chemotherapy and Clinical Research, National Cancer Center Research Institute, [b]Department of Orthopedic Surgery, Keio University, [c]BioBusiness Group, Mitsui Knowledge Industry and [d]Musculoskeletal Oncology Division, National Cancer Center Hospital, Tokyo, Japan

Key Words
MicroRNA · Osteosarcoma · Microarray · Proteomics

Abstract
Objective: Osteosarcoma (OS) is the most frequent primary malignant bone tumor in children and young adults. Although the introduction of combined neoadjuvant chemotherapy has significantly prolonged survival, the outcome for OS patients showing a poor response to chemotherapy is still unfavorable. In order to develop new therapeutic approaches, elucidation of the entire molecular pathway regulating OS cell proliferation would be desirable. ***Methods:*** MicroRNA (miRNA) are highly conserved noncoding RNA that play important roles in the development and progression of various other cancers. Using miRNA microarrays capable of detecting a known number of 933 miRNA, 108 miRNA were found to be commonly expressed in 24 samples of OS tissue and subjected to a cell proliferation assay. ***Results:*** We found that inhibition of 5 let-7 family miRNA (hsa-let-7a, b, f, g and i) significantly suppressed the proliferation of OS cells. Using a quantitative shotgun proteomics approach, we also found that the let-7 family miRNA regulated the expression of vimentin and serpin H1 proteins. ***Conclusions:*** Our present results indicate the involvement of let-7 family miRNA in regulation of the cell proliferation as well as epithelial-mesenchymal transition of OS. Thus, let-7 family miRNA may potentially provide novel targets for the development of therapeutic strategies against OS.

Introduction

Osteosarcoma (OS), although rare, is the most frequently occurring primary malignant bone tumor, affecting mainly the metaphysis of long bones in children and adolescents. Although the introduction of combination chemotherapy over the last 3 decades has greatly improved the 5-year survival rate of OS patients [1, 2], a significant proportion of them respond poorly to chemotherapy and have a high risk of local relapse or distant metastasis even after intensive chemotherapy and curative resection of the primary site [2]. Moreover, conven-

KARGER

E-Mail karger@karger.com
www.karger.com/ocl

0030–2414/14/0862–0094$39.50/0

Tesshi Yamada
Division of Chemotherapy and Clinical Research
National Cancer Centre Research Institute
5-1-1 Tsukiji, Chuo-ku, Tokyo 104-0045 (Japan)
E-Mail tyamada@ncc.go.jp

tional cytotoxic chemotherapeutic agents often cause nonspecific adverse events [3, 4]. To improve the outcome for OS patients, it is necessary to develop new therapeutics that target the molecular pathway regulating the proliferation of OS cells.

MicroRNA (miRNA) are small, noncoding RNA 21–25 nucleotides in length involved in various critical biological processes including development, differentiation, apoptosis and proliferation [5–7]. miRNA manipulate the function of genes through mRNA degradation and/or suppression of protein translation by binding to the 3′-untranslational region of RNA transcripts [6]. It is predicted that as many as 1,000 miRNA exist in the human genome [8], and thousands of human protein-encoding genes are collectively regulated by miRNA [9, 10]. Thus, the biological properties of miRNA may facilitate potential access to several human cancers, including rare sarcomas. In fact, it has been reported that miRNA play important roles as either tumor suppressor genes or oncogenes in several human cancers [7, 11].

To our knowledge, however, little is known about the expression and function of miRNA in OS [12–15]. Here we report, for the first time, the comprehensive profiling of miRNA expression in clinical OS samples. We also performed systemic functional screening to identify miRNA that are essential for the proliferation of OS cells, and found that inhibition of let-7 family miRNA exerted a significant suppressive effect on OS cell proliferation. In other malignancies, let-7 family miRNA have generally been considered to act as tumor suppressors. Therefore, let-7 family miRNA may provide potential targets for the development of novel therapeutic strategies against OS.

Table 1. Clinicopathological characteristics of 24 OS patients

	Number of patients	%
All	24	100
Gender		
Male	14	58.3
Female	10	41.7
Age		
<10 years	4	16.7
10–19 years	13	54.2
20–29 years	4	16.7
>30 years	3	12.5
Location		
Lower extremity	20	83.3
Upper extremity	2	8.3
Axial	2	8.3
Histological subtype		
Osteoblastic	19	79.2
Chondroblastic	2	8.3
Fibroblastic	2	8.3
Telangiectatic	1	4.2
Metastasis at diagnosis		
Absent	4	16.7
Present	20	83.3
Response to neoadjuvant chemotherapy		
Good	8	33.3
Poor	15	62.5
Not done	1	4.2
Local recurrence or distal metastasis		
Yes	9	37.5
No	15	62.5
Disease status		
CDF	12	50.0
NED	4	16.7
DOD	8	33.3

CDF = Chronic disease free; NED = no evidence of disease; DOD = dead of disease.

Patients and Methods

Patients and Tumor Samples

A total of 24 fresh frozen tissue samples from patients with OS were used in this study (table 1). All the tumor samples were obtained by diagnostic incisional biopsy from their primary sites prior to preoperative chemotherapy at the National Cancer Center Hospital (Tokyo, Japan) between 1996 and 2007, as described previously [16]. All of the patients concerned provided their written informed consent, authorizing the collection and use of their samples for research purposes. The study protocol for collection of samples was approved by the institutional review board of the National Cancer Center (Tokyo, Japan).

Cell Lines

U-2 OS, Saos-2, MNNG/HOS and MG-63 cell lines were purchased from the American Tissue Culture Collection (Manassas, Va., USA). HsOS-1, NOS-1, HuO-3N1, and HuO-9N2 cell lines were purchased from the Riken Bioresource Center Cell Bank (Tsukuba, Japan). All of the OS cell lines were cultured as recommended by the suppliers.

miRNA Microarray Analysis

Total RNA was isolated using ISOGEN (Nippon Gene, Tokyo, Japan) in accordance with the manufacturer's protocol. The quality of total RNA was assessed using an Agilent 2100 Bioanalyzer (Agilent Technologies, Palo Alto, Calif., USA). miRNA expression was profiled using 3D-Gene™ Human microRNA Oligo chips (Toray, Tokyo, Japan), onto which 939 probes and 3 negative controls were spotted in duplicate. The 939 probes represented 866 known human miRNA and 73 virus-originating miRNA (39 miRNA from Epstein-Barr virus, 17 miRNA from human cytomegalovirus and 17 miRNA from Kaposi's sarcoma-associated herpesvirus).

Real-Time RT-PCR

The relative expression level of selected miRNA was quantified by real-time RT-PCR. cDNA was obtained from 2 ng of total RNA using a TaqMan MicroRNA Reverse Transcription kit (Applied Biosystems, Foster City, Calif., USA). The TaqMan primer and probe set specific to each miRNA were designed by Applied Biosystems. Amplification data measured in triplicate as an increase in reporter fluorescence were collected using the ABI PRISM 7000 Sequence Detection System (Applied Biosystems). The values from the triplicate reactions were averaged and normalized to the level of RNU6B [17]. The relative expression levels of miRNA were calculated by the comparative threshold cycle method [18].

Anti-miR miRNA Inhibitor Screening

We designed and synthesized a library of anti-miR inhibitors for 108 miRNA commonly expressed in the 24 OS samples. Each cell line was seeded at 6,000 cells per well into opaque-walled 96-well plates in triplicate on the day before transfection to obtain 70% confluency. The cells were transfected with 9 pmol of anti-miR miRNA inhibitor per well using Lipofectamine 2000 (Invitrogen, Carlsbad, Calif., USA). Anti-miR Negative Control No. 1 (Applied Biosystems) was included in each assay plate to serve as a baseline. At 72 h after transfection, cell viability was measured using the CellTiter-Glo Luminescent Cell Viability Assay (Promega, Madison, Wisc., USA), and luminescence activity was measured with a GloMax 96 Microplate Luminometer (Promega), as described previously [19]. A 10-fold serial dilution of standard adenosine triphosphate (ATP) was included in each assay plate to calculate a standard curve. The mean ATP levels in triplicate wells were normalized to those of serially diluted standard ATP and nontargeting miRNA inhibitor (negative control) included in the same 96-well assay plates.

miRNA Transfection and Protein Extraction

U-2 OS cells were transfected with the let-7 family (7a, f, g or i) or Negative Control (No. 1 or 2) Pre-miR™ miRNA Precursor Molecule (Applied Biosystems) using Lipofectamine 2000 (Invitrogen). At 72 h after transfection, cell viability was quantified by the CellTiter-Glo Luminescent Cell Viability Assay, as described above. The attached cells were scraped out in ice-cold PBS, and centrifuged at 15,000 rpm for 10 min at 4°C to remove the supernatant. The resulting cell pellets were supplemented with 100 μl of 2% sodium deoxycholate (Wako Pure Chemical, Osaka, Japan) and vortexed [20, 21]. To 200 μl of the dissolved sample, 40 μl of 5 M urea, 10 μl of 1 M NH_4CO_3 and 1 μg of Sequencing Grade Modified Trypsin (Promega) were added. After incubation at 37°C for 20 h, this mixture was supplemented with 5% formic acid, vortexed and centrifuged at 15,000 rpm for 5 min at room temperature. The collected supernatant was treated with 240 μl of ethyl acetate, vortexed and centrifuged at 15,000 rpm for 5 min at room temperature again. After collecting 200 μl of the lower layer, the peptides it contained were dried with a SpeedVac Concentrator (Thermo Electron, Holbrook, N.Y., USA) and then dissolved in 40 μl of 0.1% formic acid. The protein concentrations of all protein samples were determined by Quant-iT™ Assay (Invitrogen).

Liquid Chromatography and Mass Spectrometry

Samples were randomized and measured in duplicate with a linear gradient of 0–80% acetonitrile in 0.1% formic acid at a speed 200 nl/min for 60 min using a nanoflow high-performance liquid chromatography system (NanoFrontier nLC; Hitachi High Technologies, Tokyo, Japan) connected to an electrospray ionization quadrupole time-of-flight mass spectrometer (Q-Tof Ultima; Waters, Milford, Mass., USA). Mass spectrometry (MS) peaks were detected, normalized and quantified, using the in-house 2-dimensional image-converted analysis of liquid chromatography and MS (2DICAL) software package, as described previously [22]. A serial identification (ID) number was applied to each MS peak detected (ID1–ID47,203).

Protein Identification by Tandem MS (MS/MS)

Peak lists were generated by the Mass Navigator software package version 1.2 (Mitsui Knowledge Industry, Tokyo, Japan) and searched against the Swiss-Prot database, release 57.5, using the Mascot software package version 2.2.1 (Matrix Science, London, UK). Trypsin was designated as the enzyme, and up to 1 missed cleavage was allowed. Initial peptide tolerances for precursor and fragment ions were ±0.8 and ±1.2 Da, respectively. To achieve $p < 0.05$, the score threshold was set by the Mascot algorithm, based on the size of the database used in this search. If a peptide was matched to multiple proteins, the protein name with the highest Mascot score was chosen.

Immunoblot Analysis

Anti-β-actin mouse monoclonal antibody (AC-74) was purchased from Sigma-Aldrich. Anti-vimentin (9E7E7) and serpin H1 (E1) mouse monoclonal antibodies were purchased from Santa Cruz Biotechnology (Santa Cruz, Calif., USA). The protein samples were subjected to SDS-PAGE and transferred to Immobilon-P membranes (Millipore, Billerica, Mass., USA). After 2 h of incubation with primary antibodies at room temperature and with the relevant secondary antibodies at room temperature for 1 h, blots were detected using enhanced chemiluminescence Western blotting detection reagents (GE Healthcare, Buckinghamshire, UK) [23].

Statistical Analysis

Statistical significance between subgroups was assessed using Welch's t test and the paired t test.

Results

miRNA Expression Profiles of OS

Global miRNA expression profiles were obtained from 24 OS samples and 8 OS cell lines. The clinicopathological features of the patients with OS are summarized in table 1. We found that 108 human-originated (online suppl. table S1; for all online suppl. material, see www.karger.com/doi/10.1159/000357408) and 2 virus-originated (hcmv-miR-UL70-3p and kshv-miR-K12-10a) miRNA were commonly expressed (>20 microarray-based arbitrary units) in all of the 24 OS samples examined, whereas 515 miRNA were not expressed (<20 units) in any of the OS samples (fig. 1a). miR-1826, miR-923, miR-1308, miR-451, miR-23a, let-7a, miR-23b, let-7c,

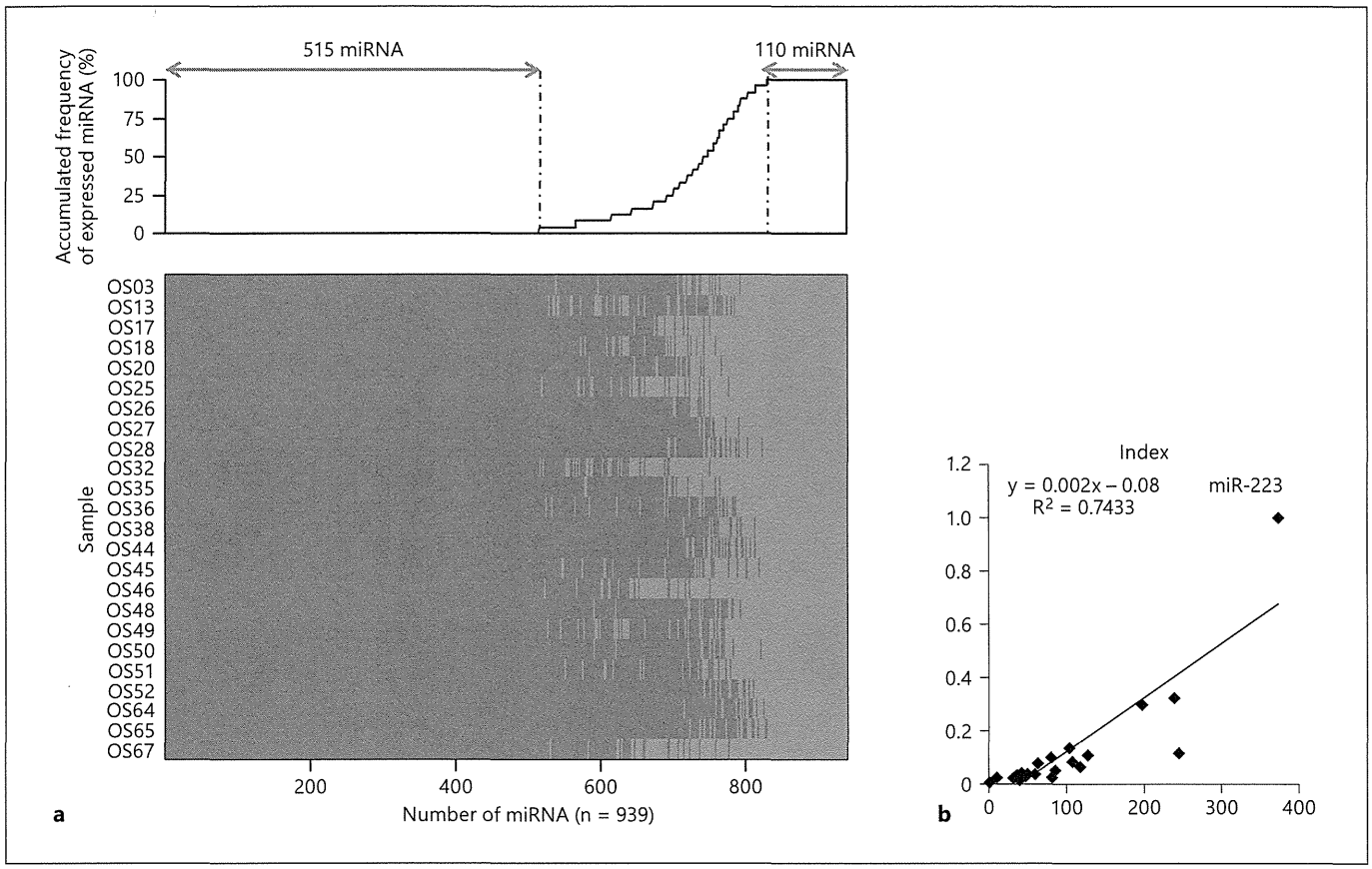

Fig. 1. Global expression of miRNA in OS. **a** The expression of 939 miRNA was examined in 24 clinical samples (range: OS03–67) using 3D-Gene miRNA microarrays. The 110 miRNA indicated by a red arrow were expressed in all the OS samples examined (>20 microarray-based arbitrary units, indicated in red columns), whereas the 515 miRNA indicated by a blue arrow were not expressed in any of them (<20 units, indicated in blue columns). **b** Correlation of miR-223 expression levels determined by microarray (x-axis, in microarray-based arbitrary units) and by quantitative real-time RT-PCR (y-axis, in arbitrary units normalized to RNU6B) in 22 OS. R = Correlation coefficient.

let-7d and miR-26a showed the highest levels of expression. The expression data on representative miRNA were also verified by real-time RT-PCR (fig. 1b and data not shown).

It was noticed that the overall profiles of miRNA expression were largely invariable among the 24 OS samples, but highly different from those of other sarcomas reported previously (data not shown), indicating that OS has an intrinsic and characteristic miRNA profile. We compared various clinicopathological characteristics, such as metastasis and prognosis, with the miRNA expression profiles. However, no definite miRNA was found to be significantly associated with the clinical behavior of the disease (data not shown), supporting the notion that OS acquires a unique miRNA expression pattern during its development.

Screening of miRNA Essential for OS Cell Proliferation

To identify miRNA essential for OS cell proliferation, we next transfected the 8 OS cell lines with synthetic inhibitors directed against the 108 miRNA of human origin, and the relative abundance of metabolically active cells was determined 72 h after transfection. The expression of the 108 miRNA and the ATP production (in percent) of the 8 OS cells transfected with these miRNA relative to control RNA are summarized in online supplementary table S1. We found that the inhibitors of 5 let-7 family miRNA (let-7a, b, f, g and i) significantly downregulated the viability of OS cells in comparison with the negative controls (fig. 2a). Conversely, the inhibitors of miR-1274a, miR-1826, miR-296-5p and miR-342-3p increased the viability of the cells. Among the 9 miRNA, the inhibitor of miR-1274a increased the average ATP pro-

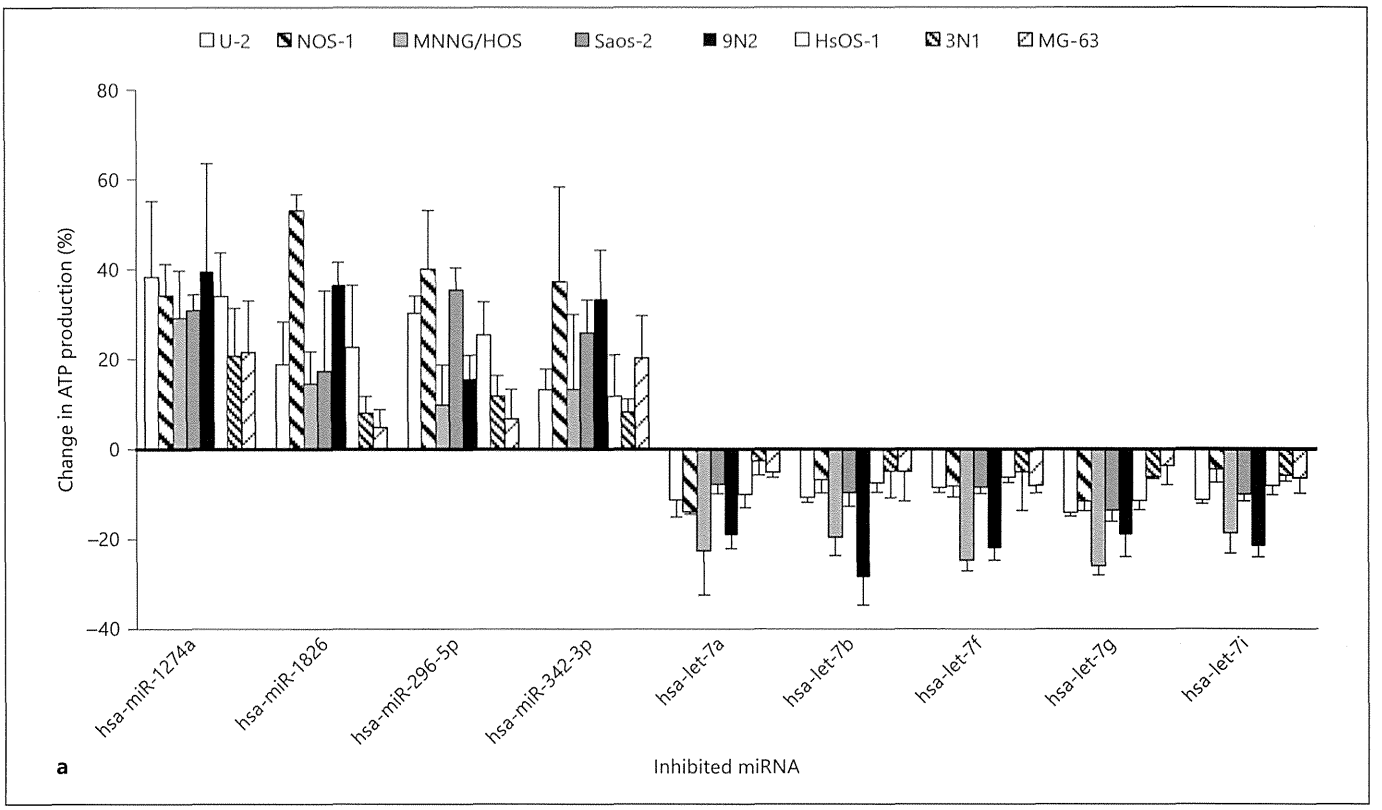

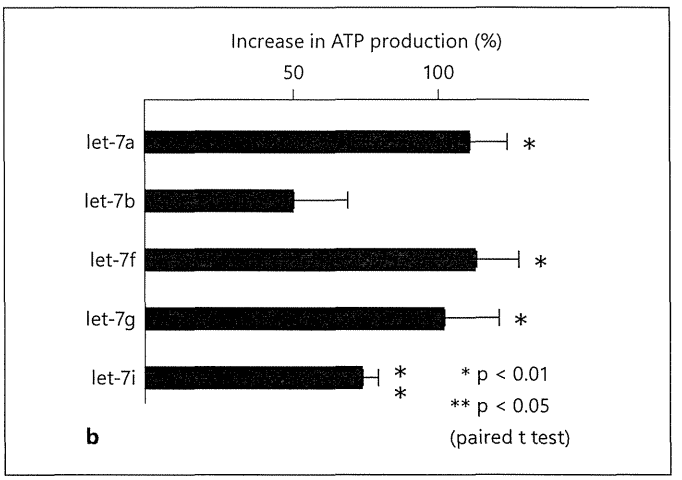

Fig. 2. Survey of miRNA regulating OS cell proliferation. **a** Percent increase (positive values) or decrease (negative values) in ATP production of 8 OS cell lines (U-2, NOS-1, MNNG/HOS, Saos-2, 9N2, HsOS-1, 3N1 and MG-63) transfected with synthetic inhibitors against miRNA. The average value of the negative control (anti-miR Negative Control No. 1) was set as 0. **b** Percent increment in ATP production in U-2 OS cells with let-7 family miRNA. The average value of the negative controls (Pre-miR miRNA Precursor Molecules, Negative Controls No. 1 and 2) was set as 0.

duction of the 8 OS cell lines (20.7–39.5% increase) and the inhibitor of let-7g reduced it (6.1–25.9% decrease; online suppl. table S1) to the maximal extent.

Transfection with let-7 Family miRNA Promotes OS Cell Proliferation

Generally, let-7 family miRNA have been considered to have tumor-suppressive functions [24]. The K-ras oncogene is one of the targets of let-7, and inhibition of let-7 increased the rate of cancer cell division, whereas overexpression of let-7 induced cell cycle arrest in the cancer cell lines [24]. However, we found that 5 of the let-7 family miRNA were commonly expressed in OS samples, and that their inhibition suppressed the viability of OS cells. To confirm these oncogenic characteristics of let-7 family miRNA in OS cells, we transfected U-2 OS cells with chemically modified, double-stranded RNA molecules designed to mimic endogenous mature miRNA of let-7a,

Table 2. Proteins regulated by let-7 family miRNA

ID	m/z	RT	Charge	Protein description	Mascot score	Peptide sequence	let-7 family	Controls	p[1]
4,893	851.0	63.7	3	serpin H1	93.14	DQAVENILVSPVVVASSLGLVSLGGK	15.24±1.96	33.31±4.41	1.71E–17
106	1,093.9	49.6	2	vimentin	73.93	EMEENFAVEAANYQDTIGR	212.34±13.97	151.14±6.40	4.30E–16
515	665.4	55.7	2	small nuclear ribonucleoprotein E	47.28	VMVQPINLIFR	86.80±5.90	62.75±2.39	3.22E–15
30,968	980.1	64.1	3	protein disulfide-isomerase	59.21	TGPAATTLPDGAAAESLVESSEVAVIGFFK	10.85±1.11	16.00±1.16	1.06E–14
324	824.4	46.6	2	heterogeneous nuclear ribonucleoprotein U	93.36	NFILDQTNVSAAAQR	114.74±9.03	75.94±8.39	3.38E–14
60	834.9	45.7	2	vimentin	54.46	ETNLDSLPLVDTHSK	267.56±19.44	195.12±7.69	3.96E–14
419	774.8	37.0	2	14-3-3 protein zeta/delta	81.66	SVTEQGAELSNEER	57.27±7.23	95.02±11.60	8.58E–14
84	867.9	44.0	2	vimentin	47.82	LQDEIQNMKEEMAR	222.70±17.28	161.62±8.15	2.53E–13
66	767.4	50.1	2	vimentin	65.19	KVESLQEEIAFLK	253.42±17.99	193.21±6.18	5.93E–13
58	794.4	39.9	2	vimentin	76.19	TNEKVELQELNDR	270.28±18.55	209.47±7.03	1.21E–12
4,771	585.9	62.9	2	vimentin	60.12	ILLAELEQLK	33.29±3.01	23.22±1.46	1.21E–12
997	759.4	55.9	3	polypyrimidine tract-binding protein 1	57.6	IAIPGLAGAGNSVLLVSNLNPER	65.10±4.57	49.00±3.38	1.57E–12
153	844.9	46.2	2	vimentin	47.24	VEVERDNLAEDIMR	171.02±14.66	124.21±5.18	2.16E–12
136	561.3	45.7	2	vimentin	52.47	EYQDLLNVK	156.93±19.07	100.58±5.15	1.20E–11
1,298	823.4	49.3	2	stress-70 protein, mitochondrial	82.19	VINEPTAAALAYGLDK	56.36±5.96	39.29±1.29	2.28E–11

Values for let-7 family and controls denote means ± SD. RT = Retention time.
[1] Welch's t test.

let-7b, let-7f, let-7g and let-7i. Again, we observed that the let-7 family miRNA significantly increased the metabolic activity of the OS cells ($p < 0.05$; fig. 2b).

Identification of Targets of let-7 Family miRNA in OS Using a Proteomics Approach

miRNA regulate the expression of target genes at the posttranscriptional level through translational inhibition as well as mRNA destabilization. One miRNA can repress the translation of hundreds of human protein-coding genes, thus exerting its distinct function. These target genes can be practically predicted, using bioinformatic approaches [10, 25, 26], but due to their relatively high rates of false positivity and negativity [6], we searched for proteins whose expression would be commonly affected by transfection with let-7 family miRNA (let-7a, let-7f, let-7g and let-7i), using an originally developed label-free quantitative MS platform: 2DICAL [22, 27].

Among a total of 47,203 independent MS peaks detected within the range of 250–1,600 m/z and within a retention time of 30–70 min, we found 253 MS peaks whose average intensity differed significantly ($p < 0.001$; Welch's t test). The intensity of 48 MS peaks was decreased in OS cells transfected with let-7 family miRNA, and that of the remaining 205 was increased. Tandem MS (MS/MS) analysis revealed that an MS peak with the highest statistical significance was derived from the *SERPINH1* (serpin H1) gene product, and the *VIM* (vimentin) gene products were detected most repeatedly (48 times) among the 253 differentially expressed MS peaks. Table 2 lists 15 MS peaks with the statistical significance of $p < 1 \times 10^{-10}$. The expression of serpin H1 was increased and that of vimentin was decreased after transfection with let-7 family miRNA. Figure 3a shows the distribution of representative serpin H1-derived and vimentin-derived MS peaks [ID 4,893 (at 851 m/z and 63.5 min) and ID 106 (at 1,094 m/z and 49.5 min), respectively] in U-2 OS cells transfected with let-7 family miRNA and controls. The differential expression and identification of serpin H1 and vimentin proteins were confirmed by immunoblotting (fig. 3b).

Discussion

Dysregulation of various miRNA has been implicated in the development and progression of human cancers. miRNA control hundreds of gene targets and play

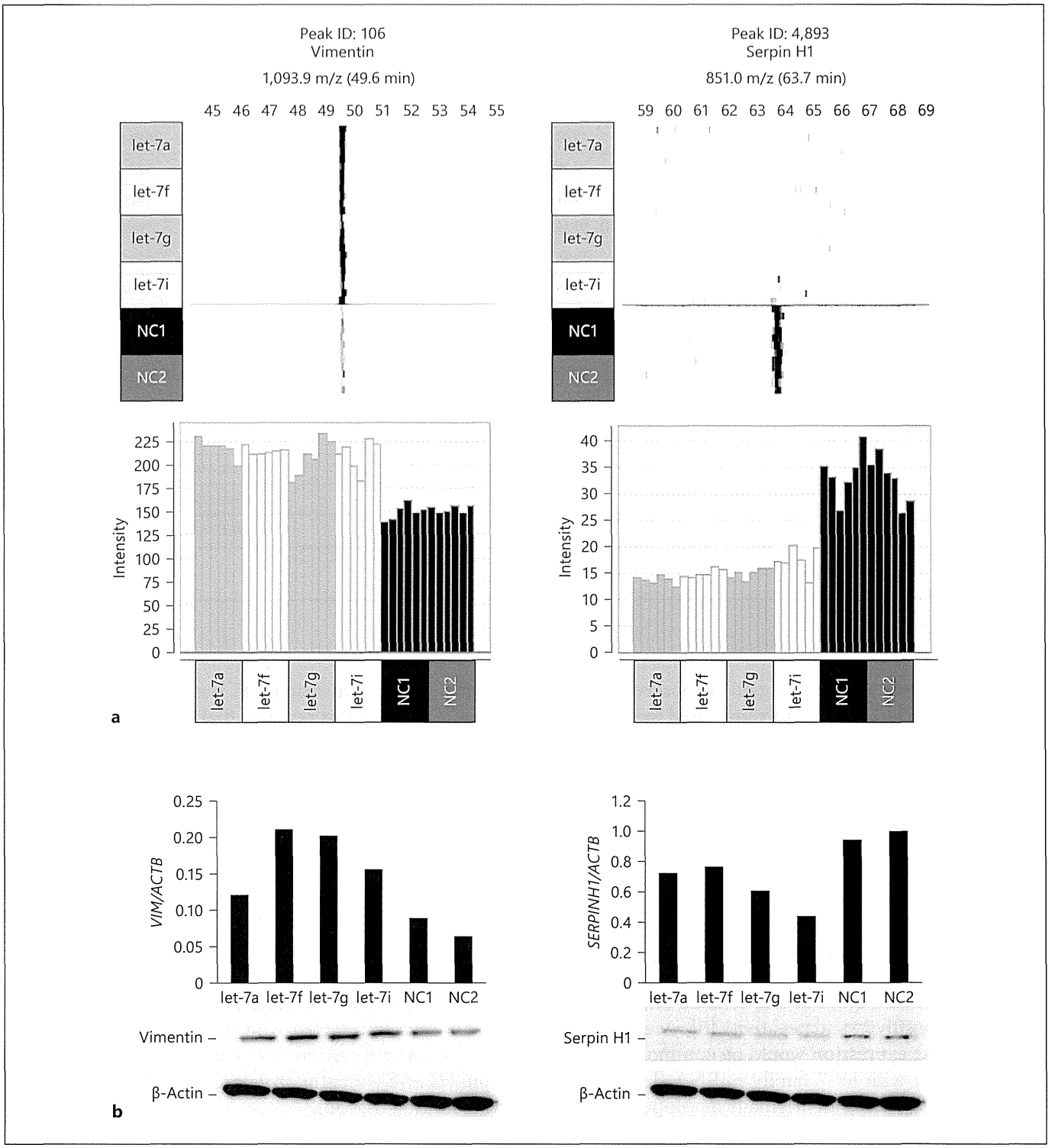

Fig. 3. Identification of proteins regulated by let-7 family miRNA. **a** Representative vimentin-derived and serpin H1-derived MS peaks detected in U-2 cells transfected with let-7 family miRNA (7a, 7f, 7g and 7i) and control RNA (NC1 and NC2). MS peaks are aligned along the retention time of liquid chromatography (in minutes). Columns: intensity (in arbitrary units) of sextuple MS peaks. **b** Detection of vimentin, serpin H1 and β-actin (loading control) in U-2 cells transfected with let-7 family miRNA (7a, 7f, 7g and 7i) and control RNA (NC1 and NC2) by immunoblotting. Columns represent the relative quantification (in arbitrary units) of vimentin *(VIM)* and serpin H1 *(SERPINH1)* normalized to β-actin *(ACTB)*.

important roles in homeostatic processes such as cell differentiation, proliferation and apoptosis [5–7]. miRNA, therefore, could be attractive candidates for the development of novel prognostic markers and/or therapeutic targets. The significance of miRNA expression has been extensively studied in various human epithelial tumors to elucidate the molecular mechanisms underlying carcinogenesis, and to identify therapeutic targets [28, 29]. However, the expression and function of miRNA in mesenchymal tumors have remained largely unknown. Subramanian et al. [30] obtained miRNA expression profiles for a series of 27 sarcomas and found distinct miRNA expression patterns for specific histopathological types, but no case of OS was included in their study. Sarver et al. [31] performed an unsupervised clustering analysis of miRNA expression in various sarcomas, including 15 cases of OS, and found that OS formed a single cluster that was distinct from other sarcomas. OS often shows a highly aggressive phenotype and lacks apparent histological differentiation, but the tissue lineage-specific regulation of miRNA expression seems to be maintained. We observed that the expression of miRNA was relatively invariable among the 24 cases of OS, regardless of their differing histological subtypes (fig. 1a). In fact we were unable to find any miRNA whose expression was significantly correlated with the clinicopathological characteristics of OS (table 1), indicating that the 108 miRNA listed in online supplementary table S1 play important roles in the development of OS.

In this study we performed an unbiased functional screening of miRNA to identify those essential for OS cell proliferation. We transfected 8 OS cell lines with miRNA inhibitors specific to the 108 miRNA commonly expressed in the 24 clinical samples, and evaluated the effects of these inhibitors on cell viability. One of the most remarkable findings was that the inhibitors of 5 let-7 family miRNA (let-7a, b, f, g and i) commonly suppressed the growth of OS cells (fig. 2a). We further confirmed these results by transfecting OS cells with let-7 family miRNA (fig. 2b). The let-7 family miRNA was originally discovered in *Caenorhabditis elegans*, and was subsequently found to be conserved in humans [32, 33]. The expression of let-7 family miRNA was reduced in various human malignancies including lung cancer, hepatocellular carcinoma, melanoma and prostate cancer [33], and the reduction in let-7 expression was associated with poor outcome in patients with lung cancer [34]. Forced expression of let-7 inhibited cell growth and downregulated multiple oncogenic proteins such as K-ras, c-Myc and HMGA2 [33, 35]. Based on these observations, let-7 family miRNA have been considered to function as tumor suppressors. However, let-7 family miRNA function differently in OS, indicating that their diverse effects are dependent on tissue lineage.

miRNA govern the expression of target proteins through mRNA degradation and suppression of protein translation [6]. Proteomics technologies have increasingly been applied for identifying the downstream targets of miRNA [36, 37]. However, the levels of alteration are often subtle and cannot be detected by conventional proteomics methods. To identify the proteins targeted by let-7 family miRNA in OS cells, we performed quantitative shotgun proteomics analysis (fig. 3a; table 2). Using the 2DICAL platform, we identified 2 let-7-responsive proteins in OS – serpin H1 and vimentin – whose expression was downregulated or upregulated, respectively, by let-7 family miRNA. In 2DICAL, whole proteins are enzymatically digested into a large array of small peptide fragments having uniform physical and chemical characteristics, and these are quantified directly by high-speed MS [22]. The 2DICAL platform is highly advantageous for clinical proteomics studies, and several cancer biomarkers have been successfully identified using this approach [27, 38, 39].

It is generally accepted that the expression of vimentin represents the mesenchymal phenotypes of various tumors, indicating that the expression of let-7 family miRNA induces OS cells to acquire mesenchymal properties, leading to an increase in tumor aggressiveness. In osteoblasts, vimentin inhibits the transactivation activity of an osteoblast-enriched transcription factor, ATF4 (activating transcription factor 4), and thus ATF4-mediated osteoblast terminal differentiation [40]. The expression of let-7 family miRNA is therefore considered to suppress the differentiation of osteoblasts and contribute to carcinogenesis. Through this osteoblast lineage-specific molecular pathway, let-7 family miRNA may exert an oncogenic function in OS cells, but not in other tumors.

Another protein that we identified as a target of let-7 family miRNA was serpin H1 (also called 'heat shock protein 47', HSP47). HSP47 is a stress-inducible collagen-binding protein that acts as a collagen-specific chaperone promoting the expression of type I collagen, which is essential for the differentiation of osteoblasts [41, 42]. Our data showed that OS cells transfected with let-7 family miRNA had reduced HSP47 expression, suggesting that this suppression of HSP47 may induce OS cells to dedifferentiate.

Conclusions

We have conducted a comprehensive functional survey of miRNA involved in the development of OS. We found that let-7 family miRNA are invariably expressed in OS and potentially contribute to OS cell proliferation and dedifferentiation. The osteoblast lineage-specific molecular pathway regulated by let-7 family miRNA could provide a novel therapeutic target for OS.

Acknowledgements

We thank Drs. Robert Nakayama and Kazutaka Kikuta (National Cancer Center Research Institute, Tokyo, Japan) for collecting samples and isolating RNA, and Ms. Sachiyo Mitani for technical assistance. E.K. is an awardee of a Research Resident Fellowship from the Foundation for Promotion of Cancer Research (Tokyo, Japan) for the Third-Term Comprehensive 10-Year Strategy for Cancer Control. Grant support was provided by the Program for Promotion of Fundamental Studies in Health Sciences conducted by the National Institute of Biomedical Innovation of Japan and the Third-Term Comprehensive Control Research for Cancer and Research on Biological Markers for New Drug Development conducted by the Ministry of Health, Labor, and Welfare of Japan.

Disclosure Statement

No potential conflicts of interest are disclosed.

References

1 Uribe-Botero G, Russell WO, Sutow WW, Martin RG: Primary osteosarcoma of bone: clinicopathologic investigation of 243 cases, with necropsy studies in 54. Am J Clin Pathol 1977;67:427–435.
2 Bielack SS, Kempf-Bielack B, Delling G, et al: Prognostic factors in high-grade osteosarcoma of the extremities or trunk: an analysis of 1,702 patients treated on neoadjuvant cooperative osteosarcoma study group protocols. J Clin Oncol 2002;20:776–790.
3 Clark JC, Dass CR, Choong PF: A review of clinical and molecular prognostic factors in osteosarcoma. J Cancer Res Clin Oncol 2008; 134:281–297.
4 Meyers PA, Schwartz CL, Krailo M, et al: Osteosarcoma: a randomized, prospective trial of the addition of ifosfamide and/or muramyl tripeptide to cisplatin, doxorubicin, and high-dose methotrexate. J Clin Oncol 2005;23: 2004–2011.
5 Ambros V: The functions of animal micro RNAs. Nature 2004;431:350–355.
6 Bartel DP: MicroRNAs: genomics, biogenesis, mechanism, and function. Cell 2004;116: 281–297.
7 Negrini M, Ferracin M, Sabbioni S, Croce CM: MicroRNAs in human cancer: from research to therapy. J Cell Sci 2007;120:1833–1840.
8 Berezikov E, Guryev V, van de Belt J, et al: Phylogenetic shadowing and computational identification of human microRNA genes. Cell 2005;120:21–24.
9 Lewis BP, Burge CB, Bartel DP: Conserved seed pairing, often flanked by adenosines, indicates that thousands of human genes are microRNA targets. Cell 2005;120:15–20.
10 Lim LP, Lau NC, Garrett-Engele P, et al: Microarray analysis shows that some micro RNAs downregulate large numbers of target mRNAs. Nature 2005;433:769–773.
11 Zhang B, Pan X, Cobb GP, Anderson TA: microRNAs as oncogenes and tumor suppressors. Dev Biol 2007;302:1–12.
12 Song B, Wang Y, Xi Y, et al: Mechanism of chemoresistance mediated by miR-140 in human osteosarcoma and colon cancer cells. Oncogene 2009;28:4065–4074.
13 Song B, Wang Y, Titmus MA, et al: Molecular mechanism of chemoresistance by miR-215 in osteosarcoma and colon cancer cells. Mol Cancer 2010;9:96.
14 Ziyan W, Shuhua Y, Xiufang W, Xiaoyun L: MicroRNA-21 is involved in osteosarcoma cell invasion and migration. Med Oncol 2011; 28:1469–1474.
15 He C, Xiong J, Xu X, et al: Functional elucidation of MiR-34 in osteosarcoma cells and primary tumor samples. Biochem Biophys Res Commun 2009;388:35–40.
16 Kobayashi E, Masuda M, Nakayama R, et al: Reduced argininosuccinate synthetase is a predictive biomarker for the development of pulmonary metastasis in patients with osteosarcoma. Mol Cancer Ther 2010;9:535–544.
17 Fukao T, Fukuda Y, Kiga K, et al: An evolutionarily conserved mechanism for microRNA-223 expression revealed by microRNA gene profiling. Cell 2007;129:617–631.
18 Huang L, Shitashige M, Satow R, et al: Functional interaction of DNA topoisomerase IIα with the β-catenin and T-cell factor-4 complex. Gastroenterology 2007;133:1569–1578.
19 Yamaguchi U, Honda K, Satow R, et al: Functional genome screen for therapeutic targets of osteosarcoma. Cancer Sci 2009;100:2268–2274.
20 Masuda T, Tomita M, Ishihama Y: Phase transfer surfactant-aided trypsin digestion for membrane proteome analysis. J Proteome Res 2008;7:731–740.
21 Ono M, Matsubara J, Honda K, et al: Prolyl 4-hydroxylation of α-fibrinogen: a novel protein modification revealed by plasma proteomics. J Biol Chem 2009;284:29041–29049.
22 Ono M, Shitashige M, Honda K, et al: Label-free quantitative proteomics using large peptide data sets generated by nanoflow liquid chromatography and mass spectrometry. Mol Cell Proteomics 2006;5:1338–1347.
23 Idogawa M, Masutani M, Shitashige M, et al: Ku70 and poly(ADP-ribose) polymerase-1 competitively regulate β-catenin and T-cell factor-4-mediated gene transactivation: possible linkage of DNA damage recognition and Wnt signaling. Cancer Res 2007;67:911–918.
24 Osada H, Takahashi T: let-7 and miR-17-92: small-sized major players in lung cancer development. Cancer Sci 2011;102:9–17.
25 Lewis BP, Shih IH, Jones-Rhoades MW, et al: Prediction of mammalian microRNA targets. Cell 2003;115:787–798.
26 Krek A, Grun D, Poy MN, et al: Combinatorial microRNA target predictions. Nat Genet 2005;37:495–500.
27 Negishi A, Ono M, Handa Y, et al: Large-scale quantitative clinical proteomics by label-free liquid chromatography and mass spectrometry. Cancer Sci 2009;100:514–519.
28 Lu J, Getz G, Miska EA, et al: MicroRNA expression profiles classify human cancers. Nature 2005;435:834–838.
29 Volinia S, Calin GA, Liu CG, et al: A micro RNA expression signature of human solid tumors defines cancer gene targets. Proc Natl Acad Sci USA 2006;103:2257–2261.
30 Subramanian S, Lui WO, Lee CH, et al: MicroRNA expression signature of human sarcomas. Oncogene 2008;27:2015–2026.
31 Sarver AL, Phalak R, Thayanithy V, Subramanian S: S-MED: sarcoma microRNA expression database. Lab Invest 2010;90:753–761.

32 Roush S, Slack FJ: The let-7 family of micro RNAs. Trends Cell Biol 2008;18:505–516.
33 Boyerinas B, Park SM, Hau A, et al: The role of let-7 in cell differentiation and cancer. Endocr Relat Cancer 2010;17:F19–F36.
34 Takamizawa J, Konishi H, Yanagisawa K, et al: Reduced expression of the let-7 micro RNAs in human lung cancers in association with shortened postoperative survival. Cancer Res 2004;64:3753–3756.
35 Lee YS, Dutta A: The tumor suppressor microRNA let-7 represses the HMGA2 oncogene. Genes Dev 2007;21:1025–1030.
36 Baek D, Villen J, Shin C, et al: The impact of microRNAs on protein output. Nature 2008; 455:64–71.
37 Selbach M, Schwanhausser B, Thierfelder N, et al: Widespread changes in protein synthesis induced by microRNAs. Nature 2008;455:58–63.
38 Matsubara J, Ono M, Negishi A, et al: Identification of a predictive biomarker for hematologic toxicities of gemcitabine. J Clin Oncol 2009;27:2261–2268.
39 Matsubara J, Ono M, Honda K, et al: Survival prediction for pancreatic cancer patients receiving gemcitabine treatment. Mol Cell Proteomics 2010;9:695–704.
40 Lian N, Wang W, Li L, et al: Vimentin inhibits ATF4-mediated osteocalcin transcription and osteoblast differentiation. J Biol Chem 2009;284:30518–30525.
41 Ragg H: The role of serpins in the surveillance of the secretory pathway. Cell Mol Life Sci 2007;64:2763–2770.
42 Nagai N, Hosokawa M, Itohara S, et al: Embryonic lethality of molecular chaperone Hsp47 knockout mice is associated with defects in collagen biosynthesis. J Cell Biol 2000; 150:1499–1506.

PHLDA3 is a novel tumor suppressor of pancreatic neuroendocrine tumors

Rieko Ohki[a,1], Kozue Saito[a,b], Yu Chen[a,b], Tatsuya Kawase[c], Nobuyoshi Hiraoka[d], Raira Saigawa[a,b], Maiko Minegishi[a,b], Yukie Aita[a], Goichi Yanai[e], Hiroko Shimizu[f], Shinichi Yachida[a], Naoaki Sakata[g], Ryuichiro Doi[h], Tomoo Kosuge[i], Kazuaki Shimada[i], Benjamin Tycko[j], Toshihiko Tsukada[k], Yae Kanai[d], Shoichiro Sumi[e], Hideo Namiki[b], Yoichi Taya[c,l], Tatsuhiro Shibata[f,2], and Hitoshi Nakagama[a,2]

Divisions of [a]Refractory Cancer Research, [c]Radiobiology, [d]Molecular Pathology, [f]Cancer Genomics, and [k]Familial Cancer Research, National Cancer Center Research Institute, Tsukiji 5-1-1, Chuo-ku, Tokyo 104-0045, Japan; [b]Graduate School of Advanced Science and Engineering, Waseda University, 3-4-1 Okubo, Shinjuku-ku, Tokyo 169-8555, Japan; [e]Department of Organ Reconstruction, Institute for Frontier Medical Sciences, Kyoto University, 53 Kawahara-cho, Shogoin, Sakyo-ku, Kyoto 606-8507, Japan; [g]Division of Hepato-Biliary-Pancreatic Surgery, Department of Surgery, Tohoku University Graduate School of Medicine, 2-1, Seiryo-machi, Aoba-ku, Sendai 980-8575, Miyagi, Japan; [h]Department of Surgery and Surgical Basic Science, Graduate School of Medicine, Kyoto University, Yoshida-Konoe-cho, Sakyo-ku, Kyoto 606-8501, Japan; [i]Hepatobiliary and Pancreatic Surgery Division, National Cancer Center Hospital, Tsukiji 5-1-1, Chuo-ku, Tokyo 104-0045, Japan; [j]Institute for Cancer Genetics, Columbia University, New York, NY 10032; and [l]Cancer Research Center of Excellence, Center for Life Sciences, National University of Singapore, Singapore 117456

Edited by Douglas Hanahan, Swiss Federal Institute of Technology Lausanne, Lausanne, Switzerland, and approved May 1, 2014 (received for review October 25, 2013)

The molecular mechanisms underlying the development of pancreatic neuroendocrine tumors (PanNETs) have not been well defined. We report here that the genomic region of the *PHLDA3* gene undergoes loss of heterozygosity (LOH) at a remarkably high frequency in human PanNETs, and this genetic change is correlated with disease progression and poor prognosis. We also show that the *PHLDA3* locus undergoes methylation in addition to LOH, suggesting that a two-hit inactivation of the *PHLDA3* gene is required for PanNET development. We demonstrate that PHLDA3 represses Akt activity and Akt-regulated biological processes in pancreatic endocrine tissues, and that *PHLDA3*-deficient mice develop islet hyperplasia. In addition, we show that the tumor-suppressing pathway mediated by MEN1, a well-known tumor suppressor of PanNETs, is dependent on the pathway mediated by PHLDA3, and inactivation of PHLDA3 and MEN1 cooperatively contribute to PanNET development. Collectively, these results indicate the existence of a novel PHLDA3-mediated pathway of tumor suppression that is important in the development of PanNETs.

p53 | PH domain | everolimus | p53 target gene | mTOR

Neuroendocrine tumors (NETs) arise from cells of the endocrine and nervous systems, and are found in tissues such as lung, pancreas and pituitary (1–3). NETs often produce, store and release biogenic amines and polypeptide hormones, and secretary granules containing these products provide a diagnostic marker for NETs. The mechanisms underlying the development of NETs remain unclear to date, due to the low incidence of these tumors and due to the lack of suitable experimental model systems, including genetically engineered mouse models. Pancreatic NET (PanNET), which is probably the best-studied NET, is the second-most common pancreatic tumor, having an incidence of ~1 per 100,000 individuals. Patients having late-stage PanNET often harbor tumors that are unresectable or metastatic and face limited treatment options. Accordingly, the prognosis of patients having metastatic PanNET is the worst among the NET subtypes, with a 5-y survival rate of 27–43% (1). Recently, the drug Everolimus has shown promise in the treatment of PanNETs (4), providing a significant improvement in progression-free survival. Everolimus is an inhibitor of mammalian target of rapamycin (mTOR), a downstream mediator of the phosphoinositide 3-kinase (PI3K)/protein kinase B (AKT) pathway. The striking efficacy of Everolimus demonstrates the importance of the PI3K/Akt pathway in the pathology of PanNETs.

In agreement with these clinical results, studies on pancreatic endocrine cell lines have identified the PI3K/Akt signaling pathway as a major proliferation and survival pathway in these cells (5). Activated Akt phosphorylates substrates such as mTOR and controls various biological processes, including protein synthesis, proliferation, cell growth, and survival. Regulation of pancreatic islet β-cell proliferation, cell size, and apoptosis by Akt has been demonstrated using various mouse models. For example, transgenic mice overexpressing constitutively active Akt in β-cells exhibit increased β-cell proliferation and cell size and decreased induction of apoptosis (6).

Recently, the results of whole exomic sequencing of 10 PanNET specimens were published, revealing several key genetic alterations (7). In particular, genes in the PI3K/Akt pathway, i.e., TSC2, PTEN, and PIK3CA, were mutated in 15% of PanNETs. However, this represents only a subset of PanNETs, and may not fully explain the remarkable clinical results achieved by Everolimus in the majority of PanNET patients.

Previously, we have shown that Pleckstrin homology-like domain family A, member 3 (PHLDA3) is a novel p53-regulated repressor of Akt. The PHLDA3 contains a PH domain that, we showed, competes with the PH domain of Akt for binding to membrane lipids, thereby inhibiting Akt translocation to the cellular membrane and its activation. We also showed that

Significance

Pancreatic neuroendocrine tumors (PanNETs) are a rare pathology, and molecular mechanisms underlying their development have not been well defined. This article shows that a two-hit inactivation of the *PHLDA3* gene is required for PanNET development: methylation of the locus and loss of heterozygosity. PHLDA3 functions as a suppressor of PanNETs via repression of Akt activity and downstream Akt-regulated biological processes. In addition, the tumor-suppressing pathway mediated by MEN1, a well known suppressor of PanNETs, is dependent on the pathway mediated by PHLDA3, and inactivation of PHLDA3 and MEN1 cooperatively contribute to PanNET development. A novel PHLDA3-mediated pathway of tumor suppression that is important in the development of PanNETs is demonstrated, and the findings may contribute to personalized medicine of PanNET patients.

Author contributions: R.O. designed research; R.O., K. Saito, Y.C., R.S., M.M., Y.A., and H.S. performed research; T. Kawase, N.H., G.Y., S.Y., N.S., R.D., T. Kosuge, K. Shimada, B.T., T.T., Y.K., and S.S. contributed new reagents/analytic tools; R.O. and K. Saito analyzed data; R.O., H. Namiki, Y.T., T.S. and H. Nakagama supervised the research; and R.O. wrote the paper.

The authors declare no conflict of interest.

This article is a PNAS Direct Submission.

[1]To whom correspondence should be addressed. E-mail: rohki@ncc.go.jp.

[2]T.S. and H. Nakagama contributed equally to this work.

This article contains supporting information online at www.pnas.org/lookup/suppl/doi:10.1073/pnas.1319962111/-/DCSupplemental.